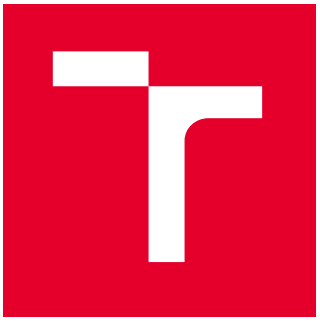

BRNO UNIVERSITY OF TECHNOLOGY

VYSOKÉ UČENÍ TECHNICKÉ V BRNĚ

FACULTY OF ELECTRICAL ENGINEERING AND COMMUNICATION

FAKULTA ELEKTROTECHNIKY
A KOMUNIKAČNÍCH TECHNOLOGIÍ

DEPARTMENT OF MICROELECTRONICS

ÚSTAV MIKROELEKTRONIKY

COILGUN

GAUSSOVA PUŠKA

BACHELOR'S THESIS
BAKALÁŘSKÁ PRÁCE

AUTHOR — **Filip Martiška**
AUTOR PRÁCE

SUPERVISOR — **Ing. Pavel Tomíček**
VEDOUCÍ PRÁCE

BRNO 2024

VYSOKÉ UČENÍ TECHNICKÉ V BRNĚ
FAKULTA ELEKTROTECHNIKY A KOMUNIKAČNÍCH TECHNOLOGIÍ

Bakalářská práce

bakalářský studijní program **Mikroelektronika a technologie**

Ústav mikroelektroniky

Student: Filip Martiška ***ID:*** 240773

Ročník: 3 ***Akademický rok:*** 2023/24

NÁZEV TÉMATU:

Gaussova puška

POKYNY PRO VYPRACOVÁNÍ:

Cílem této práce je navrhnout Gaussovu pušku. Zaměřte se na fyzikální princip funkce pušky a proveďte analýzu vlivu možných faktorů. Pomocí těchto znalostí a definovaných cílů stanovte požadavky na zařízení. Následně proveďtě samotný návrh pušky a její optimalizaci. Pušku sestavte a ověřte její funkci. Výslednou konstrukci popište v rámci bakalářské práce.

DOPORUČENÁ LITERATURA:

Podle pokynů vedoucího práce.

Termín zadání: 5.2.2024 ***Termín odevzdání:*** 30.5.2024

Vedoucí práce: Ing. Pavel Tomíček

doc. Ing. Pavel Šteffan, Ph.D.
předseda rady studijního programu

BRNO UNIVERSITY OF TECHNOLOGY
FACULTY OF ELECTRICAL ENGINEERING AND COMMUNICATION

Bachelor's Thesis

Bachelor's study program **Microelectronics and Technology**

Department of Microelectronics

Student: Filip Martiška ***ID:*** 240773

Year of study: 3 ***Academic year:*** 2023/24

TITLE OF THESIS:

Coilgun

INSTRUCTION:

The goal of this work is to design a coilgun. First study the physical background and a working principle of a coilgun and analyze different factors and their effects. Based on the background and desired parameters define requirements for the design. Next design, manufacture and optimize the coilgun.

RECOMMENDED LITERATURE:

Podle pokynů vedoucího práce.

Date of project specification: 5.2.2024 ***Deadline for submission:*** 30.5.2024

Supervisor: Ing. Pavel Tomíček

doc. Ing. Pavel Šteffan, Ph.D.
Chair of study program board

ABSTRACT

This work focuses on the coilgun, specifically the reluctance coilgun, an electromagnetic accelerator that utilizes electromagnetic induction and reluctance to propel a projectile. The initial section of this study explains the fundamental physical principles behind the coilgun's operation, including electromagnetic induction and reluctance. Following this, the work examines various design factors that influence the coilgun's performance. Finally, comprehensive measurements were conducted, a prototype was constructed, and subsequent optimizations were carried out.

KEYWORDS

Coilgun, Electromagnetic gun, Projectile Propulsion, Electromagnetism, Design Optimization, Electromagnetic Accelerator, Military Applications

ABSTRAKT

Táto práca sa zameriava na gausovu pušku, tiež známu ako reluktančná coilguna, čo je elektromagnetický urýchľovač, ktorý využíva elektromagnetickú indukciu a reluktanciu na pohon projektilu. Počiatočná časť tejto štúdie vysvetľuje základné fyzikálne princípy fungovania coilguny, vrátane elektromagnetickej indukcie a reluktancie. Následne práca skúma rôzne konštrukčné faktory, ktoré ovplyvňujú výkon coilguny. Nakoniec boli vykonané merania, postavený prototyp a uskutočnená optimalizácia.

KĽÚČOVÉ SLOVÁ

Reluktančná gausova puška, Gausova puška, Coilgun, Elektromagnetizmus, Projektilový pohon, Elektromagnetický urýchľovač, Vojenské aplikácie

ROZŠÍŘENÝ ABSTRAKT

Táto bakalárska práca sa zameriava na relatívne novú oblasť využitia elektrickej energie, konkrétne na elektromagnetický pohon, známy aj ako gausova puška alebo reluktančná coilgun.

Cieľom elektromagnetických urýchlovačov je dosiahnuť vysokú rýchlosť projektilu. Hlavné využitie tejto technológie je najmä vo vojenských aplikáciách. Existujú tri hlavné konštrukcie týchto zariadení: railgun, indukčná coilgun a reluktančná coilgun, pričom každá má svoje výhody a nevýhody.

Táto práca sa snaží podať komplexné vysvetlenie fungovania gausovej pušky a zamerať sa na základné princípy, ktoré ovplyvňujú jej funkčnosť. Taktiež sa skúma viacero konštrukčných faktorov, ktoré ovplyvňujú jej výkon, ako je napríklad konfigurácia cievky, použité materiály pre pojektil či mechanizmy na ukladanie energie. Cieľom práce je vytvoriť funkčný prototyp, ktorý bude schopný vystreliť feromagnetické projektily.

Prvá kapitola sa zaoberá základnými princípmi fungovania gausovej pušky, pričom sa venuje teórii elektrickej indukcie, magnetizmu a magnetickým poliam.

Druhá kapitola sa zameriava na vysvetlenie princípov fungovania troch najpopulárnejších elektromagnetických urýchlovačov (Railgun, indukčnej coilgun a reluktančnej coilgun) a snaží sa identifikovať problémy spojené s návrhom gausovej pušky. Napríklad sa zaoberá otázkou výberu vhodného spínacieho zariadenia, ako sú tyristor alebo IGBT, a analyzuje výhody a nevýhody každej možnosti.

Tretia časť práce je venovaná návrhu prototypu na základe predchádzajúcich teoretických úvah.

V štvrtej časti sa uskutočňujú merania a optimalizácia dizajnu. Na záver práce sú zhrnuté dosiahnuté výsledky a zhodnotenie práce.

MARTIŠKA, Filip. *Coilgun*. Bachelor's Thesis. Brno: Brno University of Technology, Fakulta elektrotechniky a komunikačních technologií, Ústav mikroelektroniky, 2024. Advised by Ing. Pavel Tomíček

Author's Declaration

Author:	Filip Martiška
Author's ID:	240773
Paper type:	Bachelor's Thesis
Academic year:	2023/24
Topic:	Coilgun

I declare that I have written this paper independently, under the guidance of the advisor and using exclusively the technical references and other sources of information cited in the paper and listed in the comprehensive bibliography at the end of the paper.

As the author, I furthermore declare that, with respect to the creation of this paper, I have not infringed any copyright or violated anyone's personal and/or ownership rights. In this context, I am fully aware of the consequences of breaking Regulation § 11 of the Copyright Act No. 121/2000 Coll. of the Czech Republic, as amended, and of any breach of rights related to intellectual property or introduced within amendments to relevant Acts such as the Intellectual Property Act or the Criminal Code, Act No. 40/2009 Coll. of the Czech Republic, Section 2, Head VI, Part 4.

Brno ....

author's signature*

*The author signs only in the printed version.

ACKNOWLEDGEMENT

Big thanks to my advisor, Ing. Pavel Tomíček! Thanks for being patient with me and helping along the way.

Contents

List of Figures

List of Tables

Introduction

This bachelor's thesis focuses on a relatively new use of electrical energy, namely electromagnetic accelerators, more specifically reluctance coilgun also known as a gauss gun.

The goal of electromagnetic accelerators is to accelerate projectile to high speed. The main use of this technology is mainly in military applications. There are three main designs of these devices: railgun, induction coilgun, and reluctance coilgun, each with its own advantages and disadvantages.

The primary aim of this thesis is to provide a comprehensive explanation of the operational principles of coilguns, with a specific focus on the fundamental mechanisms influencing their functionality. This includes an examination of various design factors that impact performance, such as coil configuration, projectile materials, and energy storage systems. The ultimate goal is to develop a functional prototype capable of firing ferromagnetic projectiles.

First chapter covers the foundational theories underpinning coilgun, including electrical induction, magnetism, and the behavior of magnetic fields. This theoretical background is essential for understanding how coilguns operate.

Second chapter provides a detailed overview of the three most popular electromagnetic accelerators: railguns, induction coilguns, and reluctance coilguns. It addresses the technical challenges associated with coilgun design, such as selecting appropriate switching devices (e.g., mechanical switch, thyristors, IGBTs . . .) and evaluates the pros and cons of each option.

Third chapter of the thesis is devoted to the design and construction of the prototype based on previous theoretical considerations.

In the fourth chapter, measurements and design optimization are carried out. At the end of the work, the achieved results and evaluation of the work are summarized.

1 Underlying theory

1.1 The magnetic field

The force on an electric charge is dependent not only on its location but also on its velocity. Every point in space is characterized by two vector quantities that determine the force on any charge. First, the electric force, described by the electric field **E** provides a force component independent of the charge's motion. Second, an additional force component, called the magnetic force, depends on the charge's velocity.

This magnetic force has a peculiar directional character. At any particular point in space, both the direction and magnitude of the force depend on the particle's direction of motion: at every instant, the force is always perpendicular to the velocity vector; additionally, at any particular point, the force is always perpendicular to a fixed direction in space (see Fig. 1.1); and finally, the magnitude of the force is proportional to the component of the velocity that is perpendicular to this unique direction. [1][3]

All of this behavior can be described by defining the magnetic field vector **B**, which specifies both the unique direction in space and the constant of proportionality with the velocity. The magnetic force can be written as $q\mathbf{v} \times \mathbf{B}$. Thus, the total electromagnetic force on a charge can be expressed as

$$\mathbf{F} = q(\mathbf{E} + \mathbf{v} \times \mathbf{B}) \tag{1.1}$$

This is called the Lorentz force.

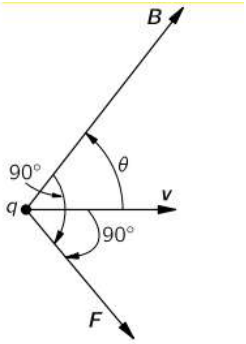

Fig. 1.1: The velocity-dependent component of the force on a moving charge is at right angles to **v** and to the direction of **B**. It is also proportional to the component of **v** at right angles to **B**, that is, to $v \sin\theta$[1]

The unit of magnetic field **B** is evidently one newton.second per coulomb-meter. The same unit is also one volt.second per $meter^2$. It is also called one *weber per square meter*.[1][3]

Electric currents consist of electrons or other charges in motion with a net drift or flow. The flow of charge can be represented by a vector that gives the amount of charge passing per unit area and per unit time through a surface element at right angles to the flow. This is called the current density and is represented by the vector **j**. It is directed along the motion of the charges. [1][3]

The total charge passing per unit time through any surface S is called the *electric current*, I. It is defined as the integral of the normal component of the flow through all the elements of the surface:

$$I = \int_S \mathbf{j} \cdot \mathbf{n} dS \tag{1.2}$$

The current consists of charged particles moving with the velocity along the wire. Each charge feels a transverse force

$$\mathbf{F} = q\mathbf{v} \times \mathbf{B} \tag{1.3}$$

If there are N such charges per unit volume, the number in a small volume ΔV of the wire is $N\,\Delta V$. The total magnetic force $\Delta\mathbf{F}$ on the volume $\Delta V$is the sum of the forces on the individual charges, that is:

$$\Delta\mathbf{F} = (N\Delta V)(q\mathbf{v} \times \mathbf{B}) \tag{1.4}$$

But Nq**v** is just **j**, so

$$\Delta\mathbf{F} = \mathbf{j} \times \mathbf{B}\ \Delta V \tag{1.5}$$

If the current is uniform across a wire with a cross-sectional area A, the volume element can be considered as a cylinder with a base area A and a length ΔL. Then:

$$\Delta\mathbf{F} = \mathbf{j} \times \mathbf{B} A \Delta L \tag{1.6}$$

Next **j**A is identified as the vector current **I** in the wire. (Its magnitude represents the electric current in the wire, and its direction is along the wire.) Then:

$$\Delta\mathbf{F} = \mathbf{I} \times \mathbf{B} \Delta L \tag{1.7}$$

This equation yields the important result that the magnetic force on a wire, resulting from the movement of charges within it, is dependent solely on the total current and not on the amount of charge carried by each particle - or even its sign.[1][3]

In the presence of a magnetic field, such as that produced by a magnet, a force acts on a wire. Following the principle of action equals reaction, one might expect that there would be a force on the source of the magnetic field, namely, on the magnet, when there is a current passing through the wire. Magnets experience forces from other magnets, indicating that when there is a current in a wire, the wire itself generates a magnetic field.

Therefore, moving charges produce a magnetic field. The validity of Maxwell's equations has been demonstrated through numerous experiments, serving as our starting point. Dropping terms involving time derivatives in these equations yields the equations of magnetostatics[1][3]

$$\nabla \cdot \mathbf{B} = 0 \tag{1.8}$$

and

$$c^2 \nabla \times \mathbf{B} = \frac{\mathbf{j}}{\epsilon_0} \tag{1.9}$$

The requirement that $\nabla \cdot \mathbf{j} = 0$ implies that only charges flowing in paths that close back on themselves are permitted. These paths, for instance, can be wires forming complete loops—referred to as circuits. Such circuits may naturally incorporate generators or batteries to maintain the flow of charges, but they cannot include charging or discharging capacitors. (The theory will later be expanded to encompass dynamic fields, but initially, is focused on steady currents.) Magnetic charges have never been discovered, so $\nabla \cdot \mathbf{B} = 0$. This holds true not just for magnetostatics but for all cases, even for dynamic fields.[1][3]

$$\oint_{\Gamma} B \cdot d\mathbf{s} = \frac{I_{through\Gamma}}{\epsilon_0 c^2} \tag{1.10}$$

This law, recognized as Ampère's law, assumes the same role in magnetostatics as Gauss' law did in electrostatics. The determination of $\mathbf{B}$ is not solely governed by Ampère's law; in general, other factors also need consideration $\nabla \cdot \mathbf{B} = 0$. [1][3]

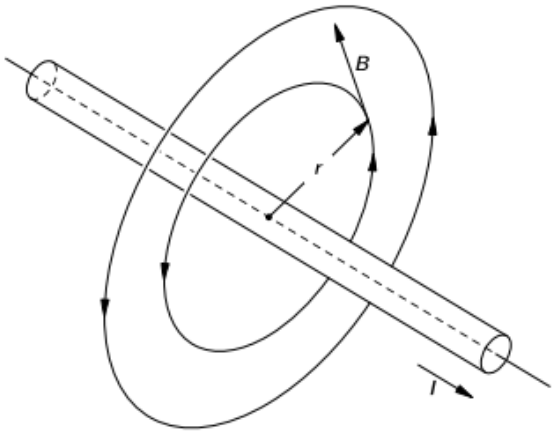

Fig. 1.2: The magnetic field outside of a long wire carrying the current I.[1]

The use of Ampère's law can be exemplified by determining the magnetic field near a wire. It will be assumed, although it may not be evident, that the field lines of **B** form closed circles around the wire. Under this assumption, Ampère's law, Eq. (1.10), provides information about the field's strength. Due to the problem's symmetry, **B** maintains the same magnitude at all points on a circle concentric with the wire (as depicted in Fig. 1.2). Consequently, the line integral of $\mathbf{B} \cdot d\mathbf{s}$ can be computed quite easily; it equals the magnitude of **B** multiplied by the circumference. If r denotes the radius of the circle, then

$$\oint_{\Gamma} B \cdot d\mathbf{s} = B \cdot 2\pi r \tag{1.11}$$

The total current through the loop is merely the current I in the wire, so

$$B \cdot 2\pi r = \frac{I}{\epsilon_0 c^2} \tag{1.12}$$

or

$$B = \frac{1}{4\pi\epsilon_0 c^2} \frac{2I}{r} \tag{1.13}$$

The strength of the magnetic field decreases inversely with r, the distance from the axis of the wire. As a magnetic field is generated by a current, it will exert a force on a nearby wire that also carries a current. If the wires are parallel, each is perpendicular to the field of the other; consequently, the wires should then be pushed either toward or away from each other. When currents flow in the same direction, the wires attract; conversely, when the currents move in opposite directions, the wires repel.[1][3]

Suppose a long coil of wire is wound in a tight spiral, as depicted by the cross sections in Fig. 1.3. Such a coil is referred to as a solenoid. It is experimentally observed that when a solenoid is much longer than its diameter, the field outside is significantly smaller than the field inside. Utilizing this observation along with Ampère's law, the size of the field inside can be determined.[1][3]

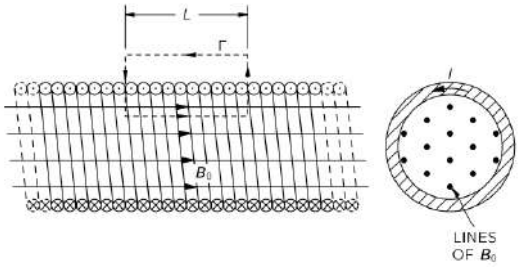

Fig. 1.3: The magnetic field of a long solenoid[1]

Since the field stays inside (and has zero divergence), its lines must go along parallel to the axis, as shown in Fig. 1.3. The line integral of $\mathbf{B}$ for this curve is just $B_0 L$, and it must be $1/\epsilon_0 c^2$ times the total current through Γ, which is NI if there are N turns of the solenoid in the length L. Thus

$$B_0 L = \frac{NI}{\epsilon_0 c^2} \tag{1.14}$$

Or, letting n be the number of turns *per unit length* of the solenoid (that is,$n = N/L$)

$$B_0 = \frac{nI}{\epsilon_0 c^2} \tag{1.15}$$

[1][3]

1.1.1 Superposition; the right-hand rule

First, basic equations for the magnetic field,

$$\nabla \cdot \mathbf{B} = 0, \qquad \nabla \times \mathbf{B} = \frac{\mathbf{j}}{c^2 \epsilon_0},$$

are linear in $\mathbf{B}$ and $\mathbf{j}$. This implies that the principle of superposition is also applicable to magnetic fields. The field generated by two distinct steady currents is the aggregate of the individual fields from each current acting independently. Our second observation concerns the right-hand rules encountered (such as the right-hand rule for the magnetic field produced by a current). Furthermore, it has been observed that the magnetization of an iron magnet arises from the spin of the electrons in the material. [1][3]

The direction of the magnetic field of a spinning electron correlates with its spin axis according to the same right-hand rule. Because $\mathbf{B}$ is determined by a "handed" rule—involving either a cross product or a curl—it is termed an axial vector. However, physically observable quantities in electromagnetism are not inherently right- (or left-) handed. Electromagnetic interactions exhibit symmetry under reflection. Consequently, when magnetic forces between two sets of currents are calculated, the outcome remains invariant with respect to a change in the hand convention. [1][3]

1.2 Induction

Upon realizing that magnetic fields are produced by electric currents, it was immediately suggested by people that, in some manner, magnets might also generate electric fields. Various experiments were conducted. For instance, two wires were arranged parallel to each other, and one of them had a current passed through it, with the hope of detecting a current in the other wire. The hypothesis was that the magnetic field might somehow induce the movement of electrons in the second wire, leading to a law akin to "likes prefer to move alike". [1][3]

Despite using the largest available current and the most sensitive galvanometer to detect any current, the outcome was negative. Similarly, large magnets placed next to wires also yielded no observed effects. Eventually, in 1840, Faraday discovered the essential feature that had been overlooked—that electric effects occur only in the presence of change. If one of a pair of wires experiences a changing current, a current is induced in the other wire, or if a magnet is moved near an electric circuit, a current arises. This phenomenon is referred to as induction, and it was discovered by Faraday.[1][3]

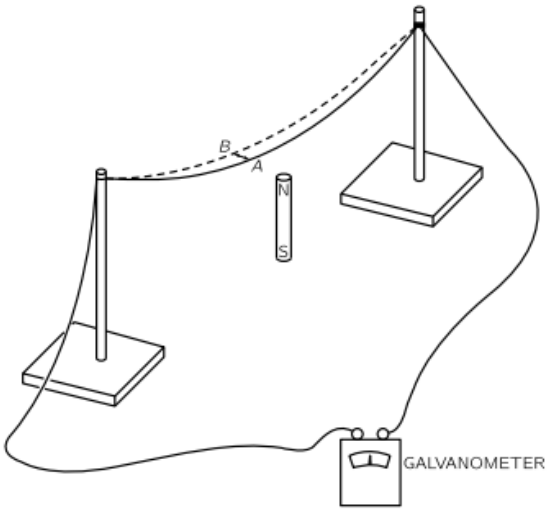

Fig. 1.4: Moving a wire through a magnetic field produces a current, as shown by the galvanometer.[1]

It is already understood that the magnetic field of a magnet originates from its internal currents. Therefore, the same effect is anticipated if, instead of a magnet in Fig. 1.4, a coil of wire with a current is used. When the wire is moved past the coil or vice versa, a current is induced through the galvanometer. However, there is now a more intriguing phenomenon: If the magnetic field of the coil is altered not by its movement but by changing its current, there is once again an effect observed in the galvanometer. For instance, if a loop of wire is positioned near a coil, as depicted in Fig. 1.5, and both are kept stationary but the current is switched off, a pulse of current is detected through the galvanometer. Upon switching the coil back on, the galvanometer responds in the opposite direction.[1][3]

Whenever the galvanometer in a situation such as the one depicted in Fig. 1.4 or Fig. 1.5 registers a current, electrons in the wire are subjected to a net push in one direction along the wire. While there may be pushes in various directions at different locations, there is a predominant push in one direction over another. What matters is the cumulative push integrated around the entire circuit. This cumulative integrated push is termed the electromotive force (abbreviated as emf) in the circuit.

More precisely, the emf is defined as the tangential force per unit charge in the wire integrated over length, once around the complete circuit. Faraday's complete discovery revealed that emfs can be generated in a wire through three different methods: by moving the wire, by moving a magnet near the wire, or by altering a current in a nearby wire. The rule dictates that when the magnetic flux passing through the loop (this flux being the normal component of $\mathbf{B}$ integrated over the area of the loop) changes with time, the emf equals the rate of change of the flux. This is referred to as "the flux rule". [1][3]

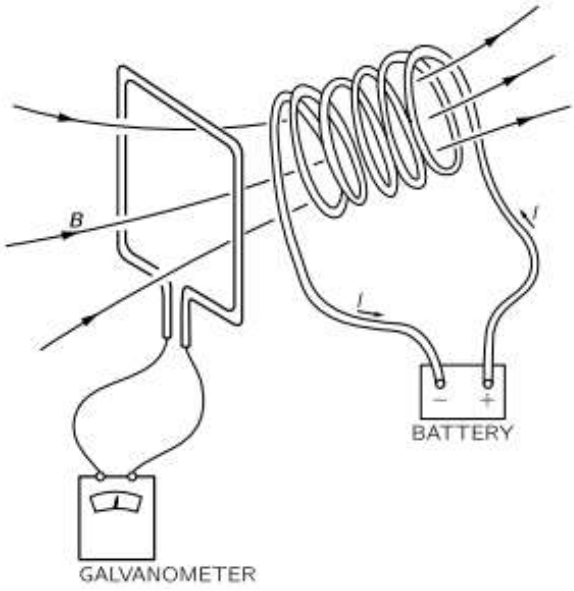

Fig. 1.5: A coil with current produces a current in a second coil if the first coil is moved or if its current is changed.[1]

One of the most intriguing features of Faraday's discoveries is not only that an emf exists in a moving coil— which can be comprehended in terms of the magnetic force $q\mathbf{v} \times \mathbf{B}$ but also that an emf is induced in a second coil by a changing current in one coil. Quite surprisingly, the amount of emf induced in the second coil is governed by the same "flux rule": the emf equals the rate of change of the magnetic flux through the coil. [1][3]

Induction effects also occur within a single coil. For example, in the setup depicted in Fig. 1.6, there is a changing flux not only through coil (b), which illuminates the bulb, but also through coil (a). The varying current in coil (a) generates a varying magnetic field within itself, causing the flux of this field to continually change. Consequently, there is a self-induced emf in coil (a). Any current experiences an emf when it is establishing a magnetic field—or, generally, when its field is changing in any manner. [1][3]

This phenomenon is referred to as self-inductance. When stating "the flux rule" that the emf equals the rate of change of the flux linkage, the direction of the emf was not specified. A straightforward rule, known as Lenz's rule, aids in determining the direction of the emf: the emf endeavors to oppose any change in flux. Thus, the direction of an induced emf is always such that if a current were to flow in its direction, it would produce a flux of $\mathbf{B}$ that opposes the change in $\mathbf{B}$ responsible for generating the emf. [1][3]

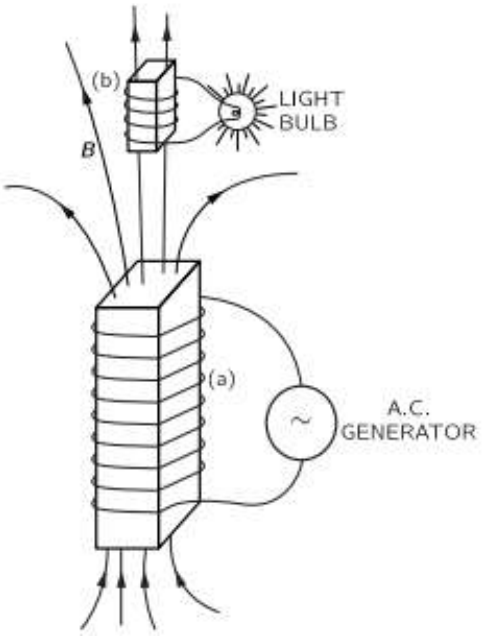

Fig. 1.6: Two coils, wrapped around bundles of iron sheets, allow a generator to light a bulb with no direct connection.[1]

Lenz's rule can be applied to determine the direction of the emf in the transformer winding of Fig. 1.5. Specifically, when there is a changing current in a single coil (or in any wire), a "back" emf occurs in the circuit. This emf acts on the charges flowing in coil (a) of Fig. 1.6 to oppose the change in magnetic field, thus opposing the change in current. It endeavors to maintain the current constant; it opposes the current when it is increasing, and aligns with the current when it is decreasing. A current in a self-inductance exhibits "inertia" because the inductive effects strive to maintain the flow constant, akin to how mechanical inertia maintains the velocity of an object constant. Any large electromagnet will possess a large self-inductance. [1][3]

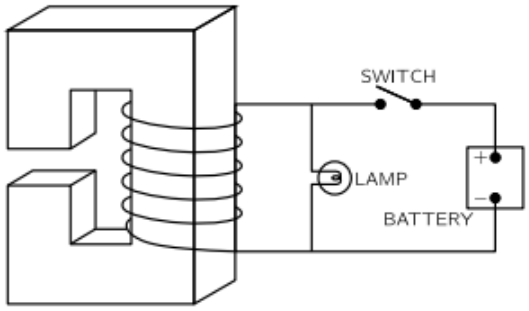

Fig. 1.7: Circuit connections for an electromagnet. The lamp allows the passage of current when the switch is opened, preventing the appearance of excessive emf's.[1]

Suppose a battery is connected to the coil of a large electromagnet, as depicted in Fig. 1.7, and a strong magnetic field has been established. (The current attains a steady value determined by the battery voltage and the resistance of the wire in the coil.) However, let us consider attempting to disconnect the battery by opening the switch. If the circuit were truly opened, the current would rapidly decrease to zero, generating an enormous emf in the process. In most scenarios, this emf would be sufficiently large to produce an arc across the opening contacts of the switch.

The resulting high voltage could potentially damage the insulation of the coil—or even harm the person opening the switch! For these reasons, electromagnets are typically connected in a circuit similar to the one depicted in Fig. 1.7. When the switch is opened, the current does not change rapidly but instead remains constant, flowing through the lamp, driven by the emf from the self-inductance of the coil.[1][3]

1.2.1 Forces on induced currents

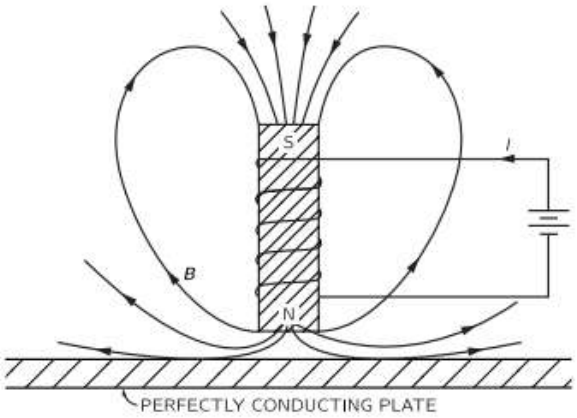

Fig. 1.8: An electromagnet near a perfectly conducting plate.[1]

If a sheet of a perfect conductor is placed next to an electromagnet and the current in the magnet is switched on, eddy currents, which are induced currents, appear in the sheet. These eddy currents serve to prevent the entry of magnetic flux. The magnet is suspended by the repulsion of the induced eddy currents in the perfect conductor. Perfect conductors are not typically found at ordinary temperatures, but some materials become perfect conductors at sufficiently low temperatures. For example, tin conducts perfectly below $3.8°K$ and is termed a superconductor.

If the conductor in Fig. 1.8 is not perfectly conductive, there will be some resistance to the flow of the eddy currents. Consequently, the currents will gradually dissipate, causing the magnet to slowly settle down. Eddy currents in an imperfect

conductor require an emf to sustain them, and for an emf to exist, the flux must continue to change. As a result, the flux of the magnetic field gradually penetrates the conductor. In a normal conductor, there are not only repulsive forces from eddy currents but also sidewise forces. For instance, if a magnet is moved sideways along a conducting surface, the eddy currents produce a drag force because the induced currents oppose the change in the location of flux. Such forces are proportional to the velocity and resemble a kind of viscous force.[1][3]

1.2.2 The physics of induction

The emf in a conducting circuit has been defined as the total accumulated force on the charges throughout the length of the loop. Specifically, it is the tangential component of the force per unit charge, integrated along the wire once around the circuit. Consequently, this quantity equals the total work done on a single charge that travels once around the circuit. The "flux rule" has also been provided, stating that the emf equals the rate at which the magnetic flux through such a conducting circuit is changing.[1][3]

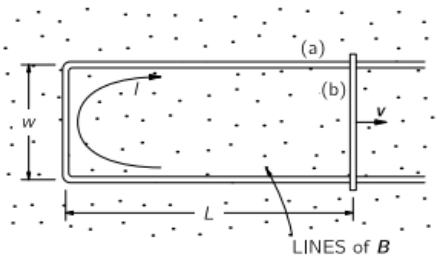

Fig. 1.9: An emf is induced in a loop if the flux is changed by varying the area of the circuit.[1]

The flux through the loop is wLB, so the "flux rule" would give, for the emf, the expression:

$$\mathcal{E} = wB\frac{dL}{dt} = wBv \tag{1.16}$$

where v is the speed of translation of the crossbar.
Now, this result from the magnetic $\mathbf{v} \times \mathbf{B}$ forces acting on the charges in the moving crossbar should be understandable. These charges will experience a force tangential to the wire, equal to vB per unit charge. It remains constant along the length w of the crossbar and is zero elsewhere, thus the integral is:

$$\mathcal{E} = wvB, \tag{1.17}$$

The same result is obtained from the rate of change of the flux.

The argument just given can be extended to any case where there is a fixed magnetic field and the wires are moved. One can prove, in general, that for any circuit whose parts move in a fixed magnetic field the emf is the time derivative of the flux, regardless of the shape of the circuit.[1][3]

The general law for the electric field associated with a changing magnetic field is

$$\nabla \times \mathbf{E} = -\frac{\partial \mathbf{B}}{\partial t} \tag{1.18}$$

Faraday's law will be referred to as such. It was discovered by Faraday but was first formulated in differential form by Maxwell, as one of his equations. The derivation of the "flux rule" for circuits from this equation will now be examined. By employing Stokes' theorem, this law can be expressed in integral form as:

$$\oint_{\Gamma} \mathbf{E} \cdot d\mathbf{s} = \int_{S} (\nabla \times \mathbf{E}) \cdot \mathbf{n}\, da \tag{1.19}$$

or

$$\oint_{\Gamma} \mathbf{E} \cdot d\mathbf{s} = -\int_{S} \frac{\partial \mathbf{B}}{dt} \cdot \mathbf{n}\, da$$

where, as usual, Γ is any closed curve and S is any surface bounded by it. Here remember, Γ is a mathematical curve fixed in space, and S is a fixed surface. Then the time derivative can be taken outside the integral and thus get

$$\oint_{\Gamma} \mathbf{E} \cdot d\mathbf{s} = -\frac{d}{dt} \int_{S} \mathbf{B} \cdot \mathbf{n}\, da \tag{1.20}$$

$$\oint_{\Gamma} \mathbf{E} \cdot d\mathbf{s} = -\frac{d}{dt}(flux\, through\, S)$$

When this relation is applied to a curve that traces a fixed circuit of conductor, the "flux rule" is obtained once again. The integral on the left represents the emf, while the integral on the right denotes the negative rate of change of the flux linked by the circuit. Thus, Eq. (1.18) applied to a fixed circuit is equivalent to the "flux rule." Therefore, the "flux rule"—stating that the emf in a circuit equals the rate of change of the magnetic flux through the circuit—applies regardless of whether the flux changes due to alterations in the field, the movement of the circuit, or both.[1][3]

It is known that the magnetic field inside a long solenoid is uniform and has the magnitude

$$B = \frac{1}{\epsilon_0 c^2} \frac{N_1 I_1}{l} \tag{1.21}$$

where N_1 is the number of turns in coil 1, I_1 is the current through it, and l is its length. Let's say that the cross-sectional area of coil 1 is S; then the flux of $\mathbf{B}$ is its

magnitude times S. If coil 2 has N_2 turns, this flux links the coil N_2 times. Therefore the emf in coil is given by

$$\mathcal{E}_2 = -N_2 S \frac{dB}{dt} \tag{1.22}$$

The only quantity in Eq. (1.21) which varies with time is I_1. The emf is therefore given by

$$\mathcal{E}_2 = -\frac{N_1 N_2 S}{\epsilon_0 c^2 l} \frac{dI_1}{dt} \tag{1.23}$$

[1][3]

1.2.3 Self-inductance

When discussing the induced electromotive forces in the two coils, only the case involving a current in one coil or the other has been considered. If currents are present in both coils simultaneously, the magnetic flux linking either coil will be the sum of the two fluxes that would exist separately, as the law of superposition applies to magnetic fields. Consequently, the emf in either coil will be proportional not only to the change in the current in the other coil but also to the change in the current of the coil itself. Thus, the total emf in the coil should be expressed.[1][3]

$$\mathcal{E}_2 = \mathfrak{M}_{21} \frac{dI_1}{dt} + \mathfrak{M}_{22} \frac{dI_2}{dt} \tag{1.24}$$

Similarly, the emf in coil 1 will depend not only on the changing current in coil 2, but also on the changing current in itself:

$$\mathcal{E}_1 = \mathfrak{M}_{12} \frac{dI_2}{dt} + \mathfrak{M}_{11} \frac{dI_1}{dt} \tag{1.25}$$

The coefficients $\mathfrak{M}_{22}$ and $\mathfrak{M}_{11}$are always negative numbers. It is usual to write

$$\mathfrak{M}_{11} = -\mathcal{L}_1, \qquad \mathfrak{M}_{22} = -\mathcal{L}_2 \tag{1.26}$$

where L_1 and L_2 are called the self-inductances of the two coils.
The self-induced emf will, of course, exist even if only one coil is present. Any coil by itself will have a self-inductance L. The emf will be proportional to the rate of change of the current in it. For a single coil, the convention is typically adopted that the emf and the current are considered positive if they are in the same direction. With this convention, the emf of a single coil may be written as:

$$\mathcal{E} = -\mathcal{L} \frac{dI}{dt} \tag{1.27}$$

The negative sign indicates that the emf opposes the change in current—it is often called a "back emf."[1][3]

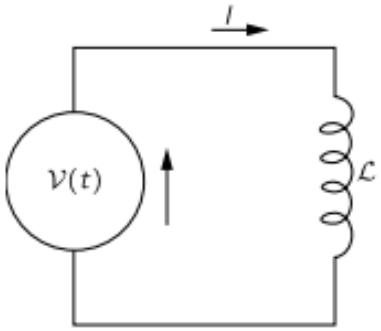

Fig. 1.10: A circuit with a voltage source and an inductance.[1]

Due to the self-inductance inherent in any coil, which opposes changes in current, the coil's current exhibits a form of inertia. Indeed, to alter the current in a coil, this inertia must be overcome by connecting the coil to an external voltage source, such as a battery or a generator, as depicted in the schematic diagram of Fig. 1.10. In such a circuit, the current I is dependent on the voltage V according to the relation:

$$V = \mathcal{L}\frac{dI}{dt} \tag{1.28}$$

[1][3]

1.2.4 Inductance and magnetic energy

It is known that the rate of electrical work by induced forces is the product of the electromotive force and the current:

$$\frac{dW}{dt} = \mathcal{E}I \tag{1.29}$$

By replacing $\mathcal{E}$ with its expression in terms of the current from Eq. (1.27), the result is:

$$\frac{dW}{dt} = -\mathcal{L}I\frac{dI}{dt} \tag{1.30}$$

Upon integrating this equation, it is found that the energy required from an external source to overcome the emf in the self-inductance while building up the current (which must equal the stored energy, U) is:

$$-W = U = \frac{1}{2}\mathcal{L}I^2 \tag{1.31}$$

Therefore the energy stored in an inductance is $\frac{1}{2}\mathcal{L}I^2$.

If the magnetic field B of a single coil is known, the self-inductance can be determined by equating the energy expression.

$$U = \frac{\epsilon_0}{2} \int \mathbf{E} \cdot \mathbf{E}\, dV \tag{1.32}$$

to $\frac{1}{2}LI^2$. Let's explore how this operates by determining the self-inductance of a long solenoid. As mentioned earlier, it has been observed that the magnetic field inside a solenoid is uniform, while outside it is zero. The magnitude of the field inside is given by $B = nI/\epsilon_0 c^2$, where n represents the number of turns per unit length in the winding and I is the current. If the radius of the coil is r and its length is L (with L assumed to be very long, allowing for the neglect of end effects, i.e., L $\gg$ r), the volume inside is $\pi r^2 L$. The magnetic energy is therefore:

$$U = \frac{\epsilon_0 c^2}{2} B^2 \cdot (Vol) = \frac{n^2 I^2}{2\epsilon_0 c^2} \pi r^2 L \tag{1.33}$$

which is equal to $\frac{1}{2}\mathcal{L}I^2$. Or,

$$\mathcal{L} = \frac{\pi r^2 n^2}{\epsilon_0 c^2} L \tag{1.34}$$

[1][3]

1.3 Maxwelll's equation

Up to this point, Maxwell's equations have been the subject of our study in fragments; it is now time to introduce one final component and amalgamate them all. Thus, the comprehensive and accurate narrative regarding electromagnetic fields that may undergo temporal changes in any manner will be obtained. There are a total of four Maxwell equations, each of which can be depicted in two distinct formats. There is the so-called integral form, which articulates the Maxwell equations using integrals, and the differential form, which articulates them using derivatives.

While the differential form of Maxwell's equations serves well for determining the magnetic and electric fields at a single point in space, the integral form is employed to compute the fields across an entire region in space. The integral form is particularly suited for resolving symmetrical problems, such as computing the electric field of a charged sphere, a charged cylinder, or a charged plane. Conversely, the differential form is more applicable for addressing complex numerical problems using computers or for deriving electromagnetic waves, for instance.

Both forms are advantageous and can be interconverted using two mathematical theorems. One theorem is termed the Divergence Integral Theorem, and the other is the Curl Integral Theorem.[1][3]

Table 1.1: Maxwell's equation

Maxwell's equations in differential form

1.	$\nabla \cdot \mathbf{E} = \frac{\rho}{\epsilon_0}$	(Flux of $\mathbf{E}$ through a closed surface) = (Charge inside)/ϵ_0
2.	$\nabla \times \mathbf{E} = -\frac{\partial \mathbf{B}}{\partial t}$	(Line integral of $\mathbf{E}$ round a loop) = -$\frac{d}{dt}$(Flux of $\mathbf{B}$ through the loop)
3.	$\nabla \cdot \mathbf{B} = 0$	(Flux of $\mathbf{B}$ through a closed surface) = 0
4.	$c^2 \nabla \times \mathbf{B} = \frac{\mathbf{j}}{\epsilon_0} + \frac{\partial \mathbf{E}}{\partial t}$	c^2(Integral of $\mathbf{B}$ around a loop) = (Current through the loop)/ϵ_0 + $\frac{d}{dt}(Fluxof\mathbf{E}throughtheloop)$

Maxwell's equations in integral form

1.	$\oint_A \mathbf{E} \cdot d\mathbf{a} = \frac{\mathbf{Q}}{\varepsilon_0}$	Gauss' Law
2.	$\oint_L \mathbf{E} \cdot d\mathbf{l} = -\frac{\partial}{\partial t} \int_A \mathbf{B} \cdot d\mathbf{a}$	Maxwell–Faraday equation (Faraday's law of induction)
3.	$\oint_A \mathbf{B}.d\mathbf{a} = 0$	Gauss's Law for magnetism
4.	$\oint_L \mathbf{B} \cdot d\mathbf{l} = \mu_0 \mathbf{I} + \mu_0 \varepsilon_0 \frac{\partial}{\partial t} \int_A \mathbf{E} \cdot d\mathbf{a}$	Ampère's circuital law (with Maxwell's addition)

Divergence integral theorem

$$\int_V (\nabla \cdot \mathbf{F}) dv = \oint_A \mathbf{F} \cdot d\mathbf{a} \tag{1.35}$$

The left side comprises the sum of the sources and sinks of the vector field within a volume, while the right side represents the total flux of the vector field through the surface of that volume. The equality between the two sides is expected.[1][3]

Therefore, the divergence integral theorem asserts that the sum of the sources and sinks of a vector field within a volume equals the flux of the vector field through the surface of that volume..[1][3]

Curl integral theorem

$$\int_A (\nabla \times \mathbf{F}) d\mathbf{a} = \oint_L \mathbf{F} \cdot d\mathbf{l}$$

The curl integral theorem states that the total curl of a vector field F within a surface A Corresponds to the rotation of the vector field F along the edge L of that surface. Well, it is somehow clear that the rotation of the vector field inside of the surface cancels in the summation and only the rotation of the vector field along the edge L remains.[1][3]

First Maxwell's equation

$$\oint_A \mathbf{E}.d\mathbf{a} = \frac{\mathbf{Q}}{\varepsilon_0} \qquad \nabla \cdot \mathbf{E} = \frac{\rho}{\epsilon_0}$$

This integral on the left hand side measures how much of the electric field comes out of or enters the surface A. The integral thus represents the electric flux through the surface A. On the right hand side is the total charge Q, which is enclosed by the surface A. Divided by the electric field constant, which provides the correct unit. The first Maxwell equation states that the electric flux phi through a closed surface A corresponds to the electric charge Q enclosed by the surface.[1][3]

Coulomb's law is a special case of the first Maxwell equation.

$$E = \frac{1}{4\pi\varepsilon_0} \frac{Q}{r^2} \tag{1.36}$$

The left-hand side of the differential form reveals the divergence of the electric field. It is understood that at a specific point in space, it can assume positive, negative, or zero values.[1][3]

The sign of the divergence determines the type of the charge at the considered point in space. If the divergence is positive, then the charge density ρ at this point in space is positive, and thus also the charge. In this point of space, there is therefore a positive charge, which is a source of the electric field. [1][3]

$$\nabla \cdot \mathbf{E}(x, y, z) > 0$$
$$\rho(x, y, z) > 0$$

If the divergence is negative, then the charge density ρ is negative, and thus also the charge. At this point of space, there is therefore a negative charge, which is a sink of the electric field.

$$\nabla \cdot \mathbf{E}(x, y, z) < 0$$
$$\rho(x, y, z) < 0$$

If the divergence is zero, then the charge density ρ is zero as well. At this point in space, there is either no charge, or there is just as much positive charge as negative, so the total charge at this point is cancelled out. At this point in space an ideal electric dipole could be located.

Maxwell equation in differential form states that the electric charges are the sources and sinks of the electric field. Charges generate the electric field. [1][3]

Second Maxwell's equation

$$\oint_L \mathbf{E} \cdot d\mathbf{l} = -\frac{\partial}{\partial t} \int_A \mathbf{B} \cdot d\mathbf{a} \qquad \nabla \times \mathbf{E} = -\frac{\partial \mathbf{B}}{\partial t}$$

On the left hand side is a line integral of the electric field E over a closed line L, which borders the surface A. This integral sums up all the parts of the electric field that run along the line L, which means it sums up how much of the electric field rotates along the line. The integral corresponds to the electric voltage U_e along the line L.

$$\oint_L \mathbf{E} \cdot d\mathbf{l} = U_e \tag{1.37}$$

$$U_e = -\frac{\partial}{\partial t} \int_A \mathbf{B} \cdot d\mathbf{a}$$

On the right side, there is a surface integral of the magnetic field B over an arbitrary surface A. This integral corresponds to the magnetic flux ϕ_m through the surface A. This magnetic flux is differentiated with respect to time t.

$$U_e = -\frac{\partial \phi_m}{\partial t} \tag{1.38}$$

So it's the temporal change of the magnetic flux. The larger the change of the magnetic flux, the greater the rotating electric field. The minus sign takes into account the direction of the rotation. If the change in the magnetic flux is positive, the electric voltage is negative. If the change in the magnetic flux is negative, the electric voltage is positive.[1][3]

The electric voltage and the change of the magnetic flux exhibit opposite behavior to each other. Energy conservation is ensured by the minus sign. Perhaps you are familiar with this principle under the name Lenz's law.[1][3]

As observed, according to this Maxwell equation, a rotating electric field gives rise to a time-varying magnetic field, and vice versa. The Lenz law now states that the magnetic flux, which is generated by the rotating electric field, counteracts its cause. Without this counteraction, the rotating electric field would amplify itself and thereby generate energy from nothing. Such an occurrence is impossible.[1][3]

In conclusion the second Maxwell equation states that the electric voltage along a closed line corresponds to the change in magnetic flux through the surface bordered by that line. In other words, a change in the magnetic flux through the surface A creates an electric voltage along the edge of A.

The second Maxwell equation in differential form states that the changing magnetic field B causes a rotating electric field E and vice versa. In such a way, that the energy conservation is fulfilled.[1][3]

Third Maxwell's equation

$$\oint_A \mathbf{B} \cdot d\mathbf{a} = 0 \qquad\qquad \nabla \cdot \mathbf{B} = 0$$

The third Maxwell equation states that there are always just as many magnetic field vectors coming out of a surface as there are vectors entering the surface.If the divergence is zero, this means that at each point in space, x, y, z, there is either no magnetic charge, also called a magnetic mono-pole. Or there is just as many positive magnetic charges as negative, so the total charge at that point cancels out.

Such as an ideal magnetic dipole, which always has both a north and a south pole. The north pole corresponds to a positive magnetic charge, and the south pole correspond to a negative magnetic charge. Since there are no magnetic mono-poles, there are no separated sources and sinks of the magnetic field.

The third Maxwell equation in differential form states that there are no magnetic mono-poles that generate a magnetic field. Only magnetic dipoles can exist.[1][3]

Fourth Maxwell's equation

$$\oint_L \mathbf{B} \cdot d\mathbf{l} = \mu_0 \mathbf{I} + \mu_0 \varepsilon_0 \frac{\partial}{\partial t} \int_A \mathbf{E} \cdot d\mathbf{a} \qquad\qquad c^2 \nabla \times \mathbf{B} = \frac{\mathbf{j}}{\epsilon_0} + \frac{\partial \mathbf{E}}{\partial t}$$

The left-hand side of the equation consists of a line integral of the magnetic field B along the closed line L. This defines the magnetic voltage U_m.

$$\oint_L \mathbf{B} \cdot d\mathbf{l} = U_m$$

On the right hand side occurs the electric field constant epsilon zero ε_0 and the magnetic field constant mu zero μ_0. They ensure that the unit on both sides of the Maxwell equation is the same.[1][3]

Additionally, a new phenomenon is observed here: the electric current I. When electric charges flow along a conductor, a current I is generated. Furthermore, there is another term: the surface integral of the electric field. This represents the electric flux through the surface A. Moreover, a time derivative precedes the electric flux. Thus, the entirety represents the temporal change of the electric flux.[1][3]

On the right side there are two summands. One contribution by the current and one contribution by the change of the electric flux. Thus, the fourth Maxwell equation states that the rotating magnetic field is generated first by the electric currents through the surface A, and second by the changing electric field.

The differential formula states that the curl of the magnetic field B at a point in space is caused in two ways. By the current density, J, and by an electric field changing at this point in space.[1][3]

1.4 Magnetism of matter

Permeability is the measure of magnetization produced in a material in response to an applied magnetic field. It is the ratio of the magnetic induction B to the magnetizing field H as a function of the field H in a material.

$$\mathbf{B} = \mu \mathbf{H} \tag{1.39}$$

$$\mu = \mu_r \mu_0 \tag{1.40}$$

Magnetic susceptibility χ is the ratio between magnetization and applied field and gives the amplification of magnetic field produced by the material.

$$\chi = \frac{\mathbf{M}}{\mathbf{H}} \tag{1.41}$$

The material with the most striking magnetic properties is, of course, iron. Similar magnetic properties are also shared by the elements nickel, cobalt, and at sufficiently low temperatures (below 16°C) by gadolinium, as well as by a number of peculiar alloys. This kind of magnetism, called ferromagnetism, is striking and complicated enough to warrant discussion in a special chapter.[1][3]

In many substances, the atoms have no permanent magnetic moments, or rather, all the magnets within each atom balance out so that the net moment of the atom is zero. The electron spins and orbital motions all exactly balance out, so that any particular atom has no average magnetic moment. In these circumstances, when a magnetic field is turned on, little extra currents are generated inside the atom by induction. According to Lenz's law, these currents are in such a direction as to oppose the increasing field. Thus, the induced magnetic moments of the atoms are directed opposite to the magnetic field. This constitutes the mechanism of diamagnetism.[1][3]

Then there are some substances for which the atoms do have a permanent magnetic moment—in which the electron spins and orbits have a net circulating current that is not zero. So besides the diamagnetic effect (which is always present), there is also the possibility of lining up the individual atomic magnetic moments. In this case, the moments try to line up with the magnetic field (in the way the permanent dipoles of a dielectric are lined up by the electric field), and the induced magnetism tends to enhance the magnetic field. These are the paramagnetic substances.[1][3]

Paramagnetism is generally fairly weak because the lining-up forces are relatively small compared with the forces from the thermal motions which try to derange the order. It also follows that paramagnetism is usually sensitive to the temperature. For ordinary paramagnetism, the lower the temperature, the stronger the effect. There is more lining-up at low temperatures when the deranging effects of the collisions are less. [1][3]

Diamagnetism, on the other hand, is more or less independent of the temperature. In any substance with built-in magnetic moments there is a diamagnetic as well as a paramagnetic effect, but the paramagnetic effect usually dominates. [1][3]

Now that a qualitative explanation of diamagnetism and paramagnetism has been attempted, it must be acknowledged that the magnetic effects of materials cannot be understood in any honest way from the point of view of classical physics. Such magnetic effects are a completely quantum-mechanical phenomenon. However, it is

possible to make some phoney classical arguments and to gain some idea of what is going on.[1][3]

1.4.1 Diamagnetism

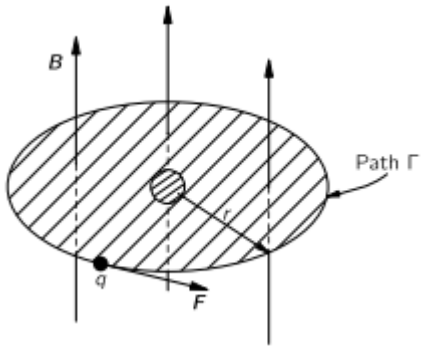

Fig. 1.11: The induced electric forces on the electrons in an atom.[1]

Next, diamagnetism will be examined from the classical point of view. It can be worked out in several ways, but one effective method is the following: Suppose that a magnetic field is slowly turned on in the vicinity of an atom. As the magnetic field changes, an electric field is generated by magnetic induction. According to Faraday's law, the line integral of **E** around any closed path equals the rate of change of the magnetic flux through the path. Consider a path Γ that is a circle of radius r concentric with the center of the atom, as shown in Fig. 1.11.[1][3]
The induced diamagnetic moment is

$$\Delta\mu = -\frac{q_e}{2m}\Delta J = -\frac{{q_e}^2 r^2}{4m}B \tag{1.42}$$

The minus sign means that the added moment is opposite to the magnetic field.

Eq. (1.42) can be written differently. The r^2 term represents the radius from an axis through the atom parallel to **B**, so if **B** is along the z-direction, it is $x^2 + y^2$. When considering spherically symmetric atoms (or averaging over atoms with their natural axes in all directions), the average of $x^2 + y^2$ is 2/3 of the average of the square of the true radial distance from the center point of the atom. Therefore, it is usually more convenient for Eq. (1.39) to be written as

$$\Delta\mu = -\frac{{q_e}^2}{6m}\langle r^2\rangle_{av}B \tag{1.43}$$

In any case, an induced atomic moment proportional to the magnetic field B and opposing it is found. This phenomenon is known as the diamagnetism of matter. [1][3]

An answer to what $\langle r^2 \rangle_{av}$ means cannot be supplied by classical mechanics. A return to quantum mechanics is necessary. In an atom, the position of an electron cannot be precisely stated, only the probability of its presence at a given location. If $\langle r^2 \rangle_{av}$ is interpreted to mean the average of the square of the distance from the center for the probability distribution, the diamagnetic moment provided by quantum mechanics aligns with formula (1.43). This equation, of course, represents the moment for one electron. The total moment is given by the sum over all the electrons in the atom. [1][3]

The surprising aspect is that the classical argument and quantum mechanics yield the same answer, although, as will be seen, the classical argument producing Eq. (1.43) is not truly valid in classical mechanics. The same diamagnetic effect occurs even when an atom already has a permanent moment. Noble gases, metalloids, metals such as Cu, Zn, and some others, and many organic compounds are diamagnetic. Additionally, all superconductors must be diamagnetic. Except for superconductors, diamagnetic materials are of low interest to engineers.[1][3]

1.4.2 Paramagnetism

Let's say just a few words about which atoms have magnetic moments and which ones don't. Any atom, like sodium for instance, which has an odd number of electrons, will have a magnetic moment. Sodium has one electron in its unfilled shell. This electron gives the atom a spin and a magnetic moment. Ordinarily, however, when compounds are formed the extra electrons in the outside shell are coupled together with other electrons whose spin directions are exactly opposite, so that all the angular momenta and magnetic moments of the valence electrons usually cancel out. That's why, in general, molecules do not have a magnetic moment.[1][3]

In chemistry, if what is called a "free radical" is present—an object with an odd number of valence electrons—then the bonds are not completely satisfied, resulting in a net angular momentum. In most bulk materials, a net magnetic moment exists only if atoms with unfilled inner electron shells are present. This can lead to a net angular momentum and a magnetic moment. Such atoms are found in the "transition element" part of the periodic table; for instance, elements such as chromium, manganese, iron, nickel, cobalt, palladium, and platinum. Additionally, all of the

rare earth elements have unfilled inner shells and permanent magnetic moments. [1][3]

Atoms in paramagnetic materials have unpaired electrons, so their spins are not compensated by paired electrons on the same quantum level. This uncompensated spin results in permanent magnetic moment, however not coupled with other atoms. Under the action of magnetic field, these moments tend to align themselves with it. Since they are not coupled together, thermal motion, which randomizes the orientation of atoms, causes magnetization to remain low with susceptibility between 10^{-6} to 10^{-3} with positive sign. Furthermore, magnetization disappears as soon as the magnetic field is removed. Paramagnetism is found in materials such as aluminium, titanium and copper alloys.Most of paramagnetic materials obey Curie's law, which means susceptibility varies inversely with absolute temperature.[1][3]

1.4.3 Ferromagnetism

The general theory of ferromagnetism, which will be used, supposes that the magnetization is caused by the spin of the electron. The electron has a spin of one-half and carries one Bohr magneton of magnetic moment, $\mu = \mu_B = q_e\hbar/2m$. The spin of the electron can be oriented either "up" or "down." Because the electron has a negative charge, a spin orientation of "up" corresponds to a negative moment, and a spin orientation of "down" corresponds to a positive moment. According to our usual conventions, the moment μ of the electron is opposite to its spin. It has been found that the energy of orientation of a magnetic dipole in a given applied field $\mathbf{B}$ is $-\mu \cdot \mathbf{B}$, but the energy of the spinning electrons also depends on the alignments of neighboring spins.[1][3]

In iron, if the moment of a nearby atom is "up" a very strong tendency exists for the moment of the adjacent atom to also be "up" This characteristic makes iron, cobalt, and nickel strongly magnetic, as the moments all align in parallel. The first question to be discussed is why this alignment occurs. Soon after the development of quantum mechanics, a very strong apparent force was noticed not a magnetic force or any other kind of actual force, but only an apparent force trying to align the spins of nearby electrons opposite to one another. These forces are closely related to chemical valence forces. [1][3]

A principle in quantum mechanics called the exclusion principle states that two electrons cannot occupy exactly the same state, they cannot be in exactly the same condition regarding location and spin orientation. For example, if they are at the

same point, the only alternative is to have their spins opposite. It is just because of the exclusion principle that electrons have a tendency to make their spins opposite. In fact, the lack of magnetism in almost all substances is explained by this principle. The spins of the free electrons on the outside of the atoms have a tremendous tendency to balance in opposite directions. The challenge is to explain why, for materials like iron, the behavior is just the reverse of what is expected.[1][3]

1.4.4 The hysteresis curve

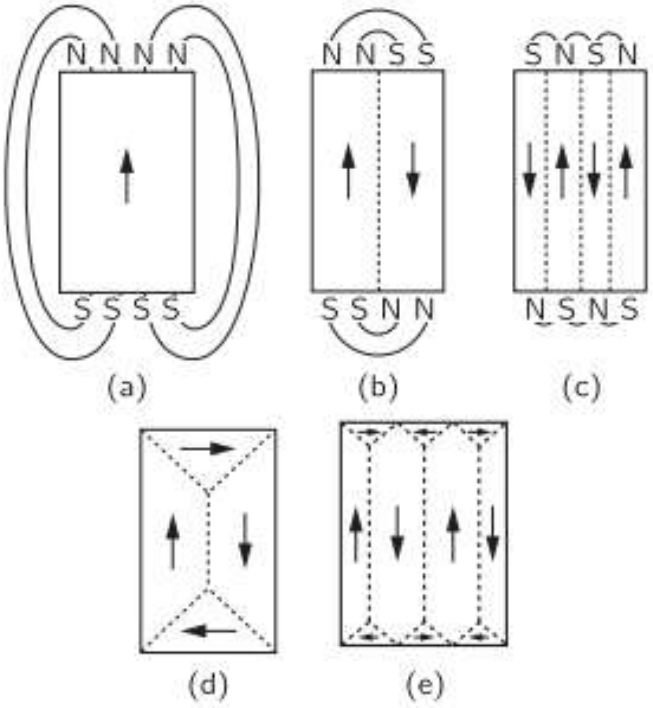

Fig. 1.12: The formation of domains in a single crystal of iron.[1]

From our theoretical analysis, it has been concluded that a ferromagnetic material should spontaneously become magnetized below a certain temperature so that all the magnetism would be in the same direction. However, it is known that this is not true for an ordinary piece of unmagnetized iron. With the help of Fig. 1.12, this phenomenon can be explained. Suppose the iron were all a big single crystal of the shape shown in Fig. 1.12(a) and spontaneously magnetized all in one direction. Then, there would be a considerable external magnetic field, which would have a lot of energy. This field energy can be reduced if it is arranged that one side of the block is magnetized "up" and the other side is magnetized "down," as shown in Fig. 1.12(b). Then, of course, the fields outside the iron would extend over less volume, resulting in less energy there.[1][3]

Ah, but wait! In the layer between the two regions, up-spinning electrons are adjacent to down-spinning electrons. However, ferromagnetism appears only in those materials for which the energy is reduced if the electrons are parallel rather than opposite. So, some extra energy has been added along the dotted line in Fig. 1.12(b); this energy is sometimes referred to as wall energy. A region having only one direction of magnetization is called a domain. At the interface—the "wall"—between two domains, where atoms on opposite sides are spinning in different directions, there is an energy per unit area of the wall. It has been described as though two adjacent atoms were spinning exactly opposite, but it turns out that nature adjusts things so that the transition is more gradual. However, such fine details need not be worried about at this point.[1][3]

Discussion will now focus on when it is better or worse to create a wall. The decision depends on the size of the domains. Suppose a block were scaled up so that the entire object doubled in size. The volume in the space outside, filled with a given magnetic field strength, would increase eightfold, and the energy in the magnetic field, which is proportional to the volume, would also increase eightfold. However, the surface area between two domains, which determines the wall energy, would only quadruple. Therefore, if the piece of iron is large enough, it will be advantageous to divide it into more domains. This is why only very tiny crystals can consist of a single domain. Any large object—more than about a hundredth of a millimeter in size—will have at least one domain wall; and any ordinary, "centimeter-size" object will be divided into many domains, as depicted in the figure. The division into domains continues until the energy required to add one extra wall becomes as large as the energy decrease in the magnetic field outside the crystal.[1][3]

Another way to reduce the energy has been discovered by nature: there is no need for the field to extend outside if a small triangular region is magnetized sideways, as shown in Fig. 1.12(d). With the arrangement depicted in Fig. 1.12(d), it is observed that there is no external field; instead, there is only a slightly larger domain wall. However, this introduces a new issue. It is found that when a single crystal of iron is magnetized, its length changes in the direction of magnetization. Thus, an "ideal" cube with its magnetization, for example, "up," is no longer perfectly cubic. The "vertical" dimension will differ from the "horizontal" dimension. This effect is known as magnetostriction.[1][3]

When an external magnetic field is applied, a crystal with domains as depicted in Fig. 1.12(d) undergoes certain changes. Initially, the middle domain wall can move sideways (to the right), reducing the energy. It shifts so that the "up" region becomes larger than the "down" region. This results in more elementary magnets aligning with the field, leading to lower energy. Consequently, for a piece of iron in weak fields, at the onset of magnetization, the domain walls start to move and encroach upon regions magnetized opposite to the field. With the field's continued increase, the entire crystal gradually shifts into a single large domain, which the external field aids in aligning. In a strong field, the crystal tends to be uniformly aligned because its energy in the applied field diminishes, it is no longer solely the crystal's own external field that holds significance. [1][3]

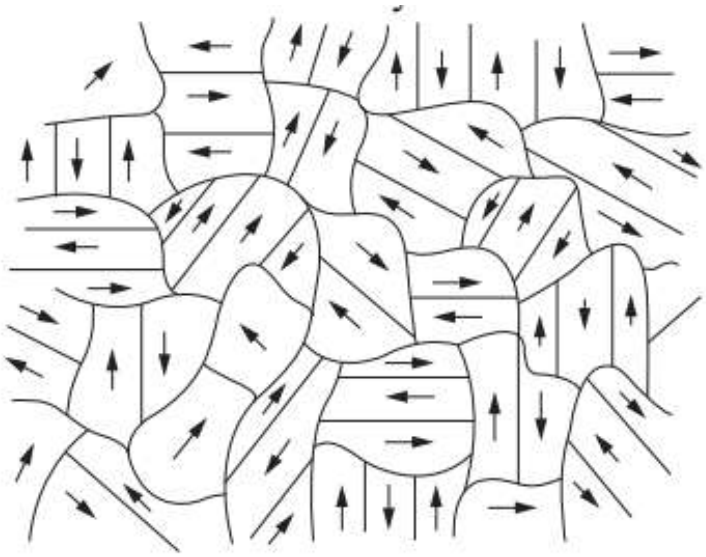

Fig. 1.13: The microscopic structure of an unmagnetized ferromagnetic material. Each crystal grain has an easy direction of magnetization and is broken up into domains which are spontaneously magnetized (usually) parallel to this direction.[1]

A polycrystalline material, such as an ordinary piece of iron, contains numerous small crystals with their crystalline axes oriented in various directions. These crystals differ from domains, which were all part of a single crystal. Within each of these crystals, there are also typically some domains. When a small magnetic field is applied to a piece of polycrystalline material, the domain walls start to move, and the domains with a favorable direction of easy magnetization expand. This expansion is reversible as long as the field remains very small; upon turning off the field, the magnetization returns to zero. This portion of the magnetization curve is labeled "a" in Fig. 1.14. [1][3]

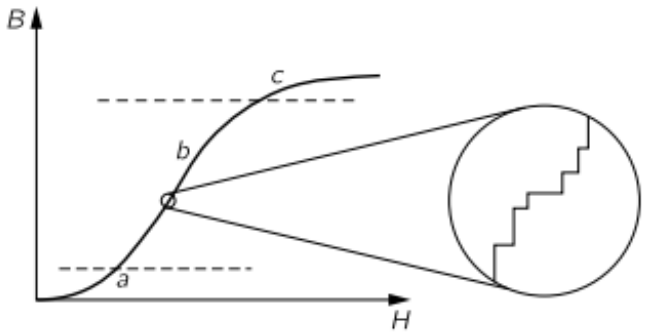

Fig. 1.14: The magnetization curve for polycrystalline iron.[1]

For larger fields—in the region b of the magnetization curve shown, things get much more complicated. In every small crystal of the material, there are strains and dislocations; there are impurities, dirt, and imperfections. And at all but the smallest fields, the domain wall, in moving, gets stuck on these. There is an interaction energy between the domain wall and a dislocation, or a grain boundary, or an impurity. So when the wall gets to one of them, it gets stuck, it sticks there at a certain field. But then if the field is raised some more, the wall suddenly snaps past. So the motion of the domain wall is not smooth the way it is in a perfect crystal, it gets hung up every once in a while and moves in jerks. If the magnetization were to be observed on a microscopic scale, a representation similar to the insert of Fig. 1.14 would be seen.[1][3]

Now the important thing is that these jerks in the magnetization can cause an energy loss. In the first place, when a boundary finally slips past an impediment, it moves very quickly to the next one, since the field is already above what would be required for the unimpeded motion. The rapid motion means that there are rapidly changing magnetic fields which produce eddy currents in the crystal. These currents lose energy in heating the metal. A second effect is that when a domain suddenly changes, part of the crystal changes its dimensions from the magnetostriction. Each sudden shift of a domain wall sets up a little sound wave that carries away energy. Because of such effects, the second part of magnetization curve is irreversible, and there is energy being lost. This is the origin of the hysteresis effect, because to move a boundary wall forward,snap and then to move it backward,snap produces a different result. It's like jerky friction, and it takes energy. [1][3]

Eventually, with sufficiently high fields, after moving all the domain walls and magnetizing each crystal in its optimal direction, some crystallites may still have their easy magnetization directions not aligned with the external magnetic field. Con-

sequently, a significant additional field is required to reorient those magnetic moments. Therefore, the magnetization gradually and smoothly increases for high fields, specifically in the region labeled "c" in the figure. The magnetization does not abruptly reach its saturation value because, in the final part of the curve, the atomic magnets are aligning in the strong field. This explains why the magnetization curve of ordinary polycrystalline materials, as depicted in Fig. 1.14, initially rises slightly and reversibly, then increases irreversibly, and eventually curves over gradually. Naturally, there is no distinct boundary between the three regions; they transition smoothly into one another.[1][3]

1.4.5 Extraordinary magnetic materials

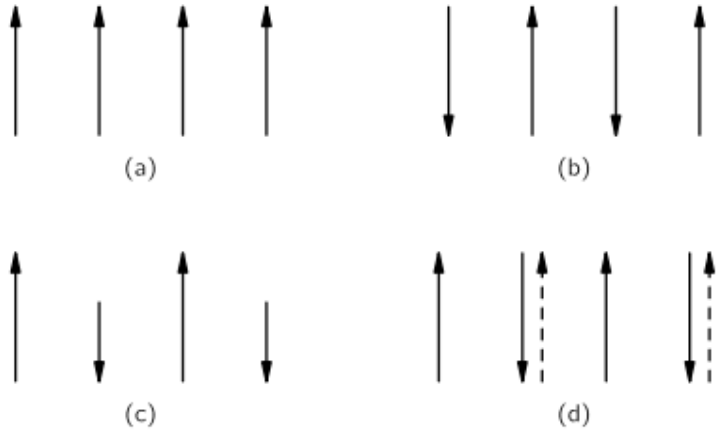

Fig. 1.15: Relative orientation of electron spins in various materials: (a) ferromagnetic, (b) antiferromagnetic, (c) ferrite, (d) yttrium-iron alloy. (Broken arrows show direction of total angular momentum, including orbital motion.)[1]

Some of the more exotic magnetic materials will now be discussed. Many elements in the periodic table possess incomplete inner electron shells and, consequently, exhibit atomic magnetic moments. For example, chromium and manganese are situated next to the ferromagnetic elements iron, nickel, and cobalt. In the chromium lattice, the spins of the chromium atoms alternate atom by atom, as depicted in Fig. 1.15(b). Therefore, chromium is considered “magnetic” from its own perspective, but it lacks significant external magnetic effects, rendering it less technically interesting. Chromium exemplifies a material where quantum mechanical effects cause the spins to alternate, classifying it as an antiferromagnetic material.[1][3]

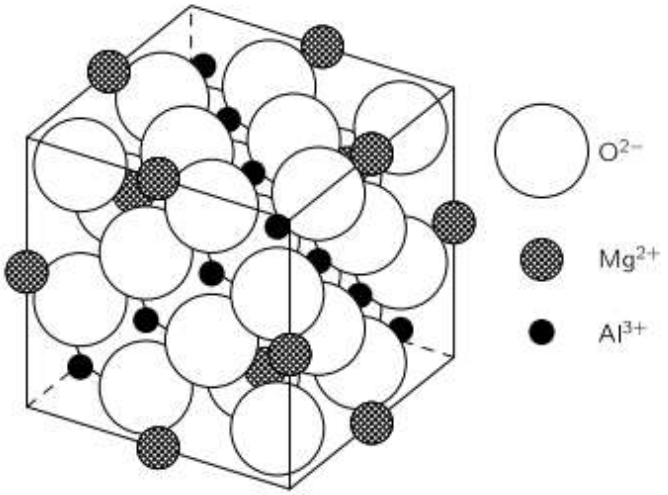

Fig. 1.16: Crystal structure of the mineral spinel ($MgAl_2O_4$); the Mg^{+2} ions occupy tetrahedral sites, each surrounded by four oxygen ions; the Al^{+3} ions occupy octahedral sites, each surrounded by six oxygen ions.)[1]

Another type of substance in which quantum mechanical effects cause electron spins to alternate but still exhibit ferromagnetism, meaning the crystal has a permanent net magnetization, will be discussed. The concept behind such materials is illustrated in Fig. 1.16. The figure depicts the crystal structure of spinel, a magnesium-aluminum oxide, which is not magnetic as shown. The oxide contains two types of metal atoms: magnesium and aluminum. When the magnesium and aluminum are replaced by two magnetic elements like iron and zinc, or zinc and manganese—essentially substituting nonmagnetic atoms with magnetic ones—an interesting phenomenon occurs. [1][3]

Labeling one type of metal atom as 'a' and the other as 'b,' the result is that all the 'a' atoms spin up and all the 'b' atoms spin down, or vice versa. However, if the magnetic moments of the 'a'-type and 'b'-type atoms are unequal, a situation like the one shown in Fig. 1.15(c) can arise, resulting in a net magnetization in the material. This material will then be weakly ferromagnetic and is known as ferrite. Although ferrites do not have as high a saturation magnetization as iron, making them useful only for smaller fields, they have a crucial difference: they are insulators. Ferrites, being ferromagnetic insulators, exhibit very small eddy currents in high-frequency fields and can thus be used in microwave systems. Unlike conductors like iron, which would block microwave fields due to eddy currents, these insulating materials allow microwave fields to penetrate. [1][3]

2 Electromagnetic launchers

Over the past century, magnetic acceleration has been the subject of extensive research and scrutiny. Electromagnetic launch technology has emerged as a competitive alternative to traditional chemically-driven propulsion systems due to its unique advantages. These launchers hold significant potential for applications in transportation, military operations, and space exploration. Electromagnetic launchers are generally categorized into two types: railguns and coilguns. [4][5]

2.1 Railgun

In a railgun, acceleration is achieved by passing a high current through the body of the projectile as it slides along a rail. This method enables the attainment of high velocities due to continuous acceleration. However, a significant drawback of this technique is the sliding contact of the high current, which causes damage to the system and reduces its lifespan.[6]

2.2 Inductance coilgun

In an inductance coilgun, there is no physical contact between the guider and the accelerated body. The system accelerates a conductive hollow cylinder projectile. The accelerated force is based on induced currents in the projectile. The induction coilgun can reach a projectile velocity of about 1000 m/s as is reported in [7].

Its advantage over the railgun is the lack of sliding high current contact. Another advantage is that a number of accelerating stages can be cascaded to reach higher projectile velocity. The main disadvantage in this method is the high induced current. This current can melt the projectile during the acceleration, which has driven the use of projectiles cooled to -196 °C.[6][8]

2.3 Reluctance coilgun

In a reluctance coilgun, as in an inductance coilgun, there is no requirement for sliding high current contacts. Furthermore, the absence of significant induced currents in the projectile prevents substantial heating, allowing for simpler projectile designs. This method also facilitates the cascading of multiple acceleration stages. Despite being the simplest method among the three discussed, the primary drawback of a reluctance coilgun is that experiments typically report much lower projectile velocities. This limitation has prompted ongoing research in the scientific community to develop reluctance coilguns capable of achieving higher velocities.[4][6][5]

The force in a reluctance coilgun is always directed towards the center of the coil. Consequently, when the projectile reaches the center during the current pulse, it experiences deceleration. Therefore, a short pulse of high current in the coil is required to achieve high velocity while avoiding deceleration, which presents conflicting demands. Additionally, precise timing is essential in a multi-stage arrangement.[8]

There are several parameters of interest for a coilgun such as projectile size and diameter, mass, kinetic energy, etc. However, one parameter above all else is the launching velocity. There are many works with simulations and compatible experiments, but still the velocity remains low. Many concepts and clever ideas were reported and checked, and improvement is seen in various parameters. But in one parameter, the velocity, no significant progress was reported. [6]

The performance of a reluctance coilgun is influenced by numerous factors, such as the number of coil turns, coil length, inner and outer coil diameters, and coil inductance. The complex interdependence of these parameters and their non-linear effects complicate accurate simulations, often resulting in significant discrepancies between experimental and simulated high-velocity outcomes. In a multi-stage reluctance coilgun, additional factors such as the timing between current pulses of each stage and the distance between stages further complicate the simulation process. [6][4]

2.4 Generic design considerations

2.4.1 Power Source

The choice of power source significantly influences performance. A battery-powered coilgun, while offering less acceleration per stage compared to capacitor-powered counterparts, presents distinct advantages and considerations. Batteries, constrained by their inability to supply as much current as capacitors, necessitate either a sizable high-current battery bank or multiple stages with smaller acceleration increments. Opting for a high-current battery bank facilitates rapid firing without the need for frequent recharging, thus streamlining operations and reducing complexity.[2][9]

On the other hand, capacitors emerge as the preferred option for maximizing raw power in a coilgun. With the capacity to be charged to exceedingly high voltages and discharged rapidly, capacitors unleash formidable energy bursts. However, a capacitor-powered coilgun requires a charging circuit. To optimize performance, each stage should be equipped with its own capacitor(s) to harness maximum voltage during firing. Preferably, multiple parallel capacitors per stage should be employed to mitigate parasitic inductance and equivalent series resistance. A well-designed coilgun would feature progressive stages with decreasing capacitance and increasing voltage, accommodating shorter yet more potent discharges in later stages.[2][9]

2.4.2 Switching

Relays/Mechanical switches

Utilizing relays or mechanical switches in coilgun design is not recommended due to their slow actuation time, typically spanning several milliseconds. While feasible, this approach compromises efficiency, which is a crucial aspect of coilgun functionality. [2]

SCR/Thyristor

SCRs (Silicon-Controlled Rectifiers) or thyristors are widely favored for their capability to handle high current loads with ease. However, once activated, these devices cannot be deactivated until the current flow ceases.(This is only true for normal thyristors. GTOs, as opposed to normal thyristors, are fully controllable switches which can be turned on and off by their gate lead.)

This limitation restricts their compatibility to capacitor-powered coilguns and necessitates meticulous control over the capacitance/resistance of each stage to achieve optimal pulse length. Neglecting this aspect often results in suboptimal exit velocities despite high voltage and current levels. Alternative strategies, such as early stage firing to ensure capacitor discharge before projectile alignment, pose further efficiency challenges.[9][2]

MOSFET/IGBT

MOSFETs and IGBTs offer precise control over pulse length, making them appealing options for coilgun applications. However, to guarantee dependable performance, additional components are necessary. These include snubber circuits to prevent semiconductor failure caused by back-EMF during sudden turnoff, as well as gate drivers to facilitate rapid and complete switching. When selecting between an IGBT and a MOSFET for a coilgun application, several factors need to be considered. IGBTs are typically more robust and can handle higher voltages and currents, making them well-suited for high power applications. On the other hand, MOSFETs have the advantage of higher switching speeds. However, given the high voltage and current requirements of a coilgun, IGBTs are generally the better choice. Additionally, IGBTs tend to be more cost-effective for the same current and voltage ratings. [2][9]

Recoil

When MOSFETs or IGBTs are utilized, significant voltage spikes are generated due to current induced by the collapsing magnetic field of the coil during their abrupt turn-off. Handling this issue is commonly achieved by employing a fly-back diode. However, this results in slower ramp-down and freewheeling of the coil. To suppress coil freewheeling, a flyback diode can be combined in series with a resistor or a reverse-bias zener diode.[2][9][4]

2.4.3 Timing

Sensors

Controlling stages with sensors is an approach that avoids the need for manual calculations or timing adjustments. However, it is strongly recommended that sensors be constructed in a manner that allows for forward/backward adjustment to achieve optimal timing. Due to the ramp-down time of coils, wherein their magnetic field dissipates gradually, positioning a sensor to intercept a projectile precisely in the center of the coil can result in deceleration of the projectile as the field dissipates.[9][2]

Regarding sensor type, optical sensors emerge as the sole viable option due to their minimal latency, typically several nanoseconds compared to several milliseconds for induction sensors. It is important to acknowledge that when firing, induced electromagnetic interference occurs in the sensors, as demonstrated by reference [6]. This interference can be mitigated with appropriate precautions, such as twisting the sensor wires with the ground wire to suppress unwanted voltage spikes.[9][2]

Software

Relying on software timing appears to be the optimal approach for achieving precise and adjustable timing of stages. However, timing adjustments will need to be redone whenever modifications are made to capacitors, coils, or projectiles. Ideal timing can be determined through simulation or trial and error. It is recommended to develop multiple timing profiles that can be switched between, particularly if adjustments to voltages or projectiles are planned.[9]

For this task, a FPGA or MCU is suitable, with the choice between them being a matter of personal preference.

Combination of both

The utilization of both sensors and a software delay is deemed advantageous. A dynamic timing system can be achieved, allowing adaptation between each stage to rectify any simulation errors and prevent the retarding of the projectile due to the suck back effect("Suck back" refers to the phenomenon where current continues to flow through the coil after the projectile has passed the midpoint.). However, the implementation of this approach is rather complex.

2.4.4 Coils

Wire thickness

The 'Field Constant', which refers to the rate at which the field strength increases per ampere flowing through the coil, is influenced by wire thickness. When the supply voltage and dimensions of two coils are identical, a coil with thicker wire will ultimately generate a stronger magnetic field. Conversely, a coil with thinner wire will produce a magnetic field more efficiently, resulting in a stronger field per ampere of current flowing through it.

Wire thickness must also be taken into account concerning the intended voltage of the coilgun. For low-voltage coilgun construction, thicker wire is preferred to ensure that the coils experience the highest possible current, thereby producing the

strongest field. However, in high-voltage gun setups, the use of thick wire may lead to exceeding the current limits for the switching devices.[9][8]

Volume

The volume of a coil is directly associated with its RL time constant, which determines the duration it takes for the coil to ramp up to maximum current (maximum field) and down to zero current. Irrespective of other factors, a larger coil will require more time to reach its maximum current and field compared to a smaller coil. Importantly, it will also take longer for its field to dissipate when switched off. This can lead to the retardation of the projectile after it has passed through the center, where the field should have dissipated. Compensating for this involves turning off the coils earlier, although this is not ideal as it misses the window of time when the projectile experiences maximum acceleration near the middle.[9]

While the notion of always opting for small coils may seem enticing, they draw exponentially more current due to lower resistance, and sometimes a coil can be too fast for the projectile's speed. An ideal coil gun will utilize progressively smaller coils with faster time constants, allowing for the most efficient acceleration up to a high speed.[9]

Width

Wider coils (width denoting the coil's diameter) are deemed undesirable. When comparing two coils with identical wire thickness, length, and supply voltage, the wider coil will exhibit a slower RL time constant, generate a weaker magnetic field, and possess a lower field constant compared to the narrower coil.[9]

The reason for not utilizing coils only one layer thick is attributed to the current draw. A coil with only one layer may have a low resistance resulting in a high current draw. Such high current levels would likely damage the majority of affordable switching devices. Therefore, careful consideration is needed to balance wire thickness and coil width to achieve the desired current draw. [9]

Length

A field extending further outward is produced by a longer coil, albeit with an overall weaker intensity. Consequently, a projectile experiences steadier acceleration. One advantage of a longer coil manifests at its center, where the force on the projectile undergoes a transition and initiates deceleration. In a longer coil, this transition is more gradual, rendering a gun employing longer coils more forgiving regarding imprecise timing of the stages.[9][6]If length of the coil and armature are the same, the efficiency reaches maximum.[4]

Temperature

The resistance of copper undergoes a change of approximately 4% per 10°C. As the magnetic field of a coil scales with its current draw, when coils heat up to 35°C, they will only generate 96% of their normal magnetic field, while cooling them to 0°C will result in the production of 110% of their normal magnetic field.[5][9]

Number of stages

Diminishing returns on speed will be yielded by adding additional coils/stages if not optimized. A reduction in the complexity, size, and cost of the gun will be achieved by focusing on having a small number of highly optimized and powerful stages.[6][9]

Current draw

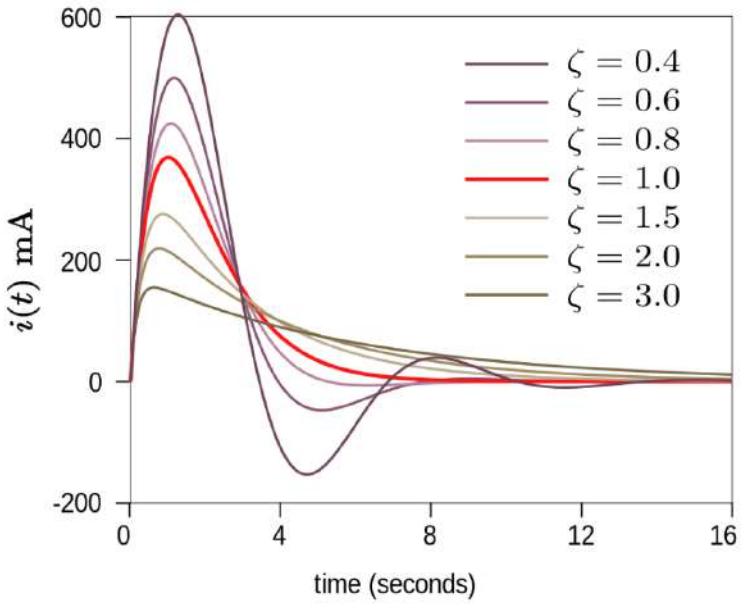

Fig. 2.1: Plot showing underdamped and overdamped responses of a series RLC circuit to a voltage input step of 1 V. The critical damping plot is the bold red curve. The plots are normalised for L = 1, C = 1 and $\omega_0 = 1$.[2]

All the aforementioned factors can be adjusted to achieve a target current draw for a given coil. It is also important to note that the circuit essentially operates as an RLC oscillator. By critically damping the circuit, the risk of charging the electrolytic capacitors to opposite polarity and damaging them is avoided. However, a critically damped circuit is undesirable because it delivers only 36% of the maximum possible peak current compared to an undamped circuit[8][9][2].

Experiments conducted by [5] demonstrate significant disparities between the actual and calculated current in a circuit, primarily due to increased inductance as the projectile enters the coil.

2.4.5 Projectile

Projectile mass

Due to the diminishing returns on speed associated with additional coils, and the increasing difficulty in rapidly turning a coil on/off, it is noteworthy that higher muzzle energy can often be achieved by launching a more massive projectile at a slower speed. [6][9][2]

Projectile length

Similar to coil length, a smoother acceleration is achieved with a longer projectile, resulting in a more gradual transition from acceleration to deceleration upon reaching the middle of a coil. Empirical experiments and simulations suggest that a practical design approach is to select a coil length ranging from the projectile length to twice the projectile length. A longer projectile can partially compensate for imprecise timing, albeit within certain limits.[4][9][2][8]

Projectile width and material

A wider projectile will consistently encounter greater force from a coil. This is attributed to the increased cross-sectional area, resulting in more metal atoms within the magnetic field's reach when the projectile is positioned near the coil's center. However, adhering to the square-cube law reveals an optimal range. Doubling the projectile's width quadruples its mass, necessitating four times the force for equivalent acceleration rates. Another variable affected by varying projectile width is the saturation flux. When a projectile reaches saturation, amplifying the strength of an external magnetic field leads to diminishing returns on the force exerted on the projectile.[9][2]

Another variable impacted by varying projectile width is the saturation flux. When a projectile reaches saturation, amplifying the strength of an external magnetic field results in diminishing returns on the force exerted on the projectile.

Therefore, implementing a projectile with high saturation flux and high magnetic permeability is advantageous when constructing a high-power coilgun. Materials such as silicon iron boron, iron DT4C, cobalt alloys and other alloys with similar properties. These materials can potentially offer higher saturation flux densities, enhancing the performance of the coilgun. Adjusting the projectile and coil widths allows a larger projectile to accommodate the same flux amount at a lower density, thereby remaining below its saturation flux density. [9][2][5][4][6]

2.4.6 Barrel

Thickness

The necessity of a rigid and low-friction barrel is evident; however, the thickness of the barrel is also crucial, particularly because the coils are wound around it. Any space between the interior of the coil and the projectile diminishes the number of magnetic field lines interacting with the projectile. Therefore, it is essential to minimize the wall thickness of a barrel without compromising its structural integrity.[9]

Material

While the choice of a metal barrel may initially seem appealing, it will diminish the efficiency of the coilgun due to the induction of eddy currents in the metal by the coils. Additionally, metal poses a risk of short-circuiting the coils, given the high voltage potential between the innermost layer of wire and the metal barrel.[9]

Carbon fiber or glass emerge as the preferred materials, given their rigidity, heat resistance, and non-conductivity. Glass offers an additional advantage of transparency, enabling the placement of optical sensors without the need for drilling holes in the barrel. [9]

3 Design and construction of two stage prototype

Requirements for the prototype are quite simple. A working coilgun which shoots ferromagnetic projectiles. The proposed prototype which tries to take into account all the design considerations is presented in this chapter. The number of stages was carefully determined based on budget constraints. Since the funding for this project was personally financed, I could only afford two stages, excluding any provisions for potential failures.

3.1 System Overview and Operation of a Multi-Stage Coilgun

The entire system can be divided into three main sections: the main power circuit, the charging circuit, and the control system. Control system does not interact in any way with the charging circuit and vice versa. To shield the low-voltage components within the control system from potential harm caused by substantial voltage spikes within the main power circuit, a isolation strategy has been implemented. This isolation is achieved optically, ensuring that voltage surges within the main power circuit are prevented from propagating to the control system. Hence, signal transmission from the control system is facilitated exclusively through optical channels.

The charging circuit is responsible for charging all the capacitors in the main power circuit to the desired voltage. Once the capacitors are charged, the charging circuit is galvanically disconnected from the main power circuit using a relay.

Upon activation of the firing switch, the control system sends a pulse of predefined length via an optical system to the first stage IGBT driver. This pulse activates the IGBT, allowing current to flow through the coil. As current flows through the coil, it generates a magnetic field that draws the projectile into the center of the coil, thereby accelerating it.

When the pulse from the control system ends, the IGBT is turned off, and the excess current is dissipated in the snubber circuit. At this point, the projectile has traversed the first stage and proceeds to the next stage. As the projectile disrupts a light barrier, the control system detects this signal and activates the second stage in the same manner as the first stage. This process could be iteratively repeated for each subsequent stage, with each stage being sequentially activated as the projectile advances through the coilgun, ensuring continuous acceleration.

3.2 Main power circuit

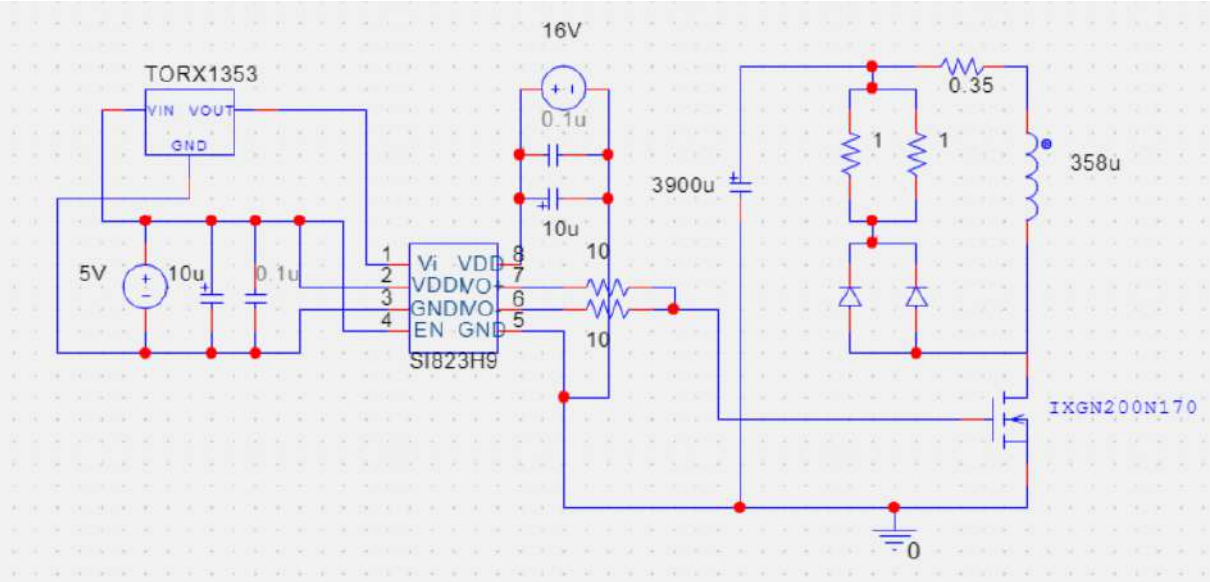

Fig. 3.1: Main power circuit

Design

Main power circuit consists of:

- Coil: R = 0.35 Ω, L = 358 μH, N = 145, Number of coils (stages) = 2
- (Power source): Electrolytic capacitors - 400V 3900uF
- (Snubber): Diode SDA100N18B-SIR, 2x50W 1Ω
- (Switch): IGBT - IXGN200N170
- IGBT driver: Si823H9AC-IS
- Optical reciver - TORX1353
- 16 V power source - 4x INR18650-25R Li-ion batteries
- 5 V power source - Modified power adapter

Capacitors utilized in this project were repurposed from a previous undertaking. This choice was driven by practical considerations of resource efficiency and cost-effectiveness.

The IGBT was chosen over the MOSFET due to its superior current handling capabilities, higher voltage tolerance, and lower cost. These attributes make the IGBT more suitable for the high-demand operational conditions required by the coilgun.

Coil Design: The length of the coil was calculated based on the length of the projectile. To ensure optimal efficiency, the coil length should be between 1 to 2 times the length of the projectile. Given that the projectile is 40 mm long, the coil length was chosen to be 60 mm.

Next the inner diameter of the coil was designed to be slightly larger than the projectile to accommodate a small gap and the barrel. This ensures smooth movement of the projectile through the barrel without significant friction or obstruction.

For winding the coil, 1 mm copper enameled wire was selected. The coil resistance was set to 0.35Ω to limit the maximum current.

An online calculator was used to determine the number of turns and the inductance of the coil.[10]

- Length = 60 mm
- Inner diameter = 18 mm
- Wire diameter = 1 mm
- Number of turns = 145
- Resistance = 0.35 Ω
- Inductance = 0.358 μH

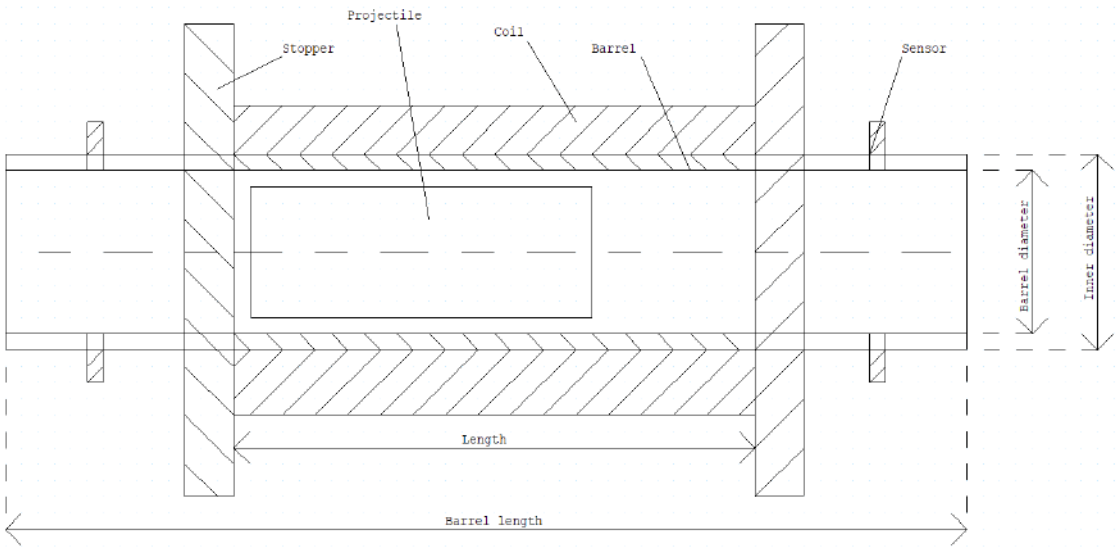

Fig. 3.2: Coil dimensions

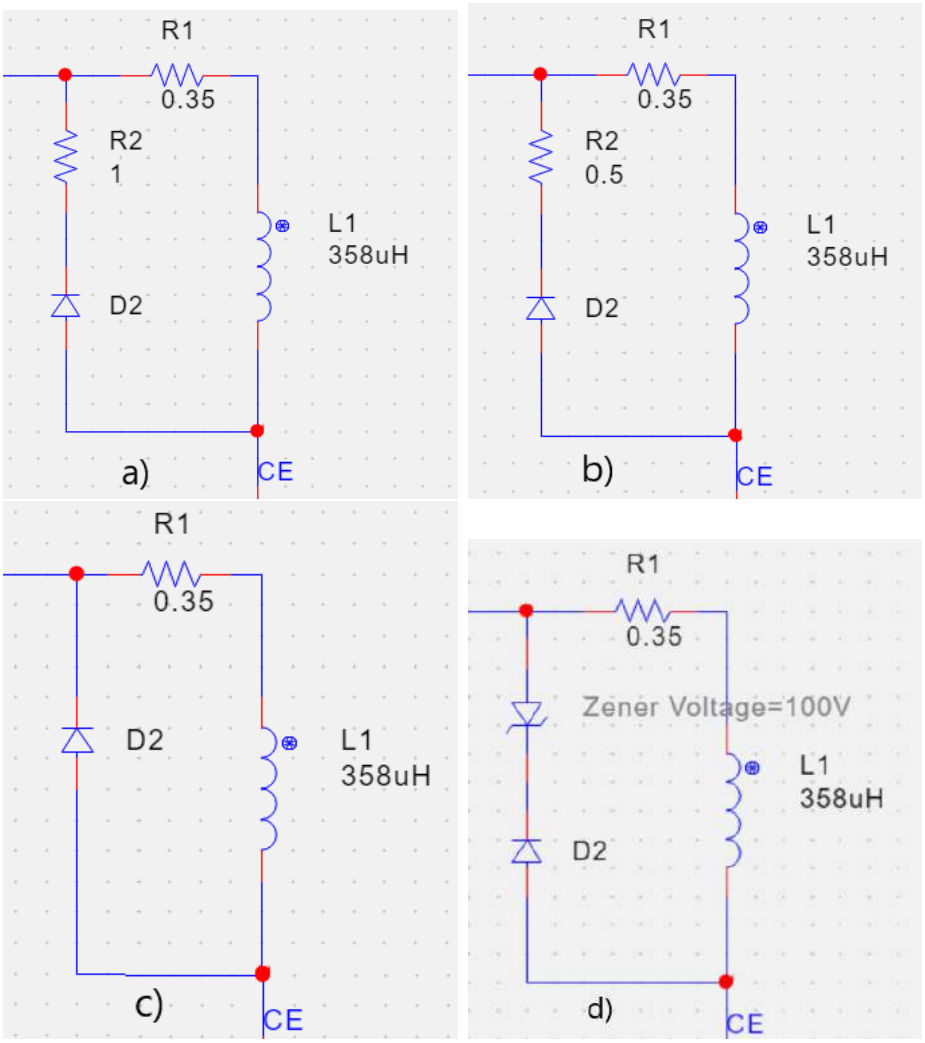

Fig. 3.3: Different considered snubbers a)diode and a 1 Ω resistor, b)diode and a 0.5 Ω resistor, c)diode d)zenner diode

Snubber circuit was designed to achieve the fastest possible discharge rate without compromising the integrity of the IGBT. The design balances the need for rapid energy dissipation with the necessity of protecting the switching device from potential damage due to voltage spikes. With previous considerations and data from simulations from Fig 3.4 in mind snubber circuit with 0.5 Ω resistor and diode was chosen.

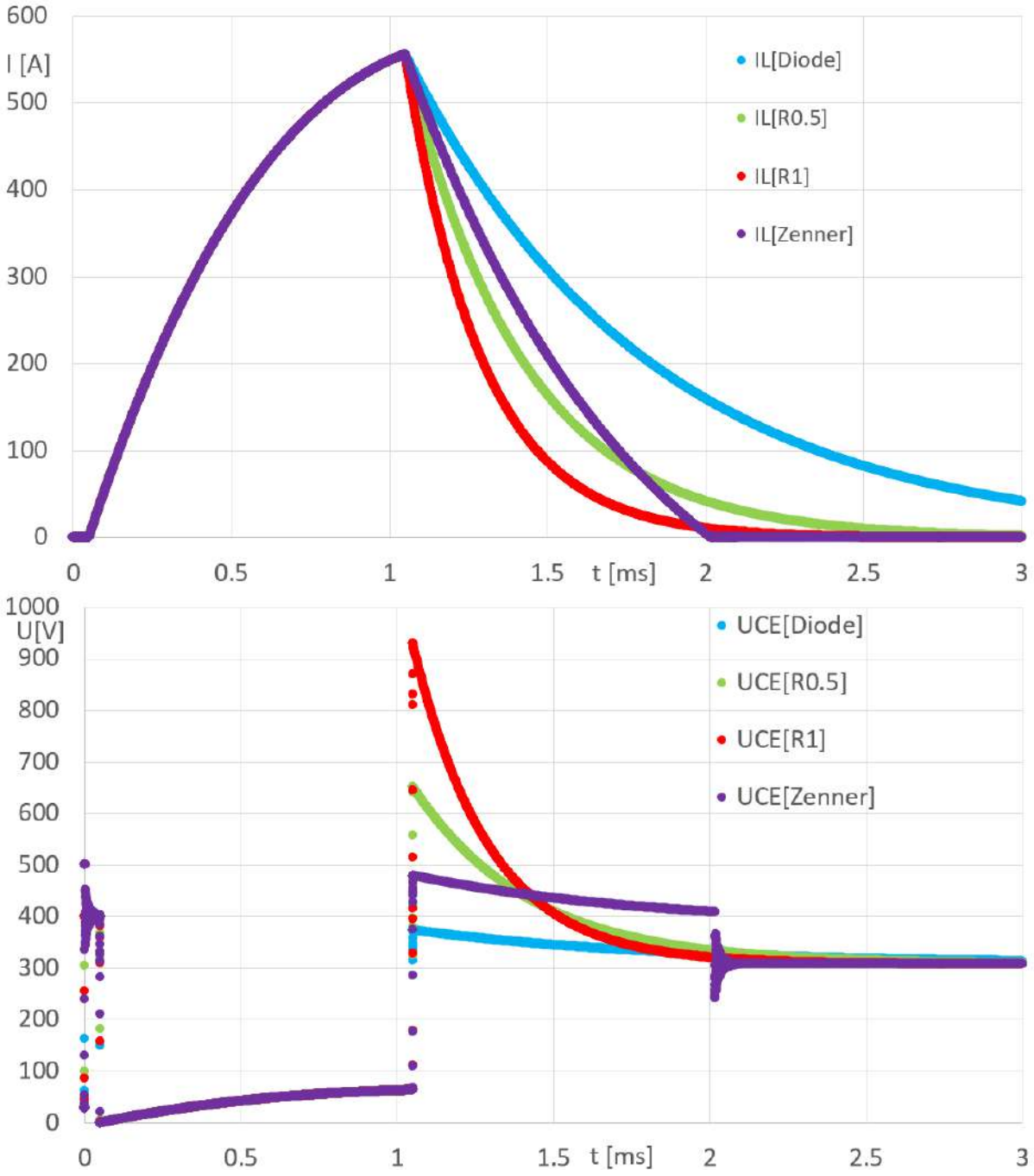

Fig. 3.4: Simulation of current discharge and voltage spike upon turnoff for snubbers (a,b,c,d) from Fig. 3.2

Construction

- Barrel length = 110 mm
- Material = PET-G
- Inner diameter of barrel = 14 mm
- Outer diamer of barrel = 18 mm

The main body of the coilgun consists of a coil, barrel, a base plate, stoppers, and arms connecting the barrel to the base plate and supporting it, all of which were fabricated via 3D printing. The coils were meticulously and painstakingly hand-wound onto the barrel. Stoppers were fixed on both ends to prevent the coil from shifting or unwinding. The length of the single stage, or more precisely, the length of a single barrel, was carefully designed to accommodate all essential components while allowing a margin of space for operational adjustments.

To mitigate the risk of unwinding due to tension, adhesive was applied to secure the coil in place. Alignment of the two stages was achieved by aligning the base plates, thereby ensuring alignment of the barrels. Subsequently, these base plates were affixed to a large plywood sheet and firmly secured using bolts and nuts.

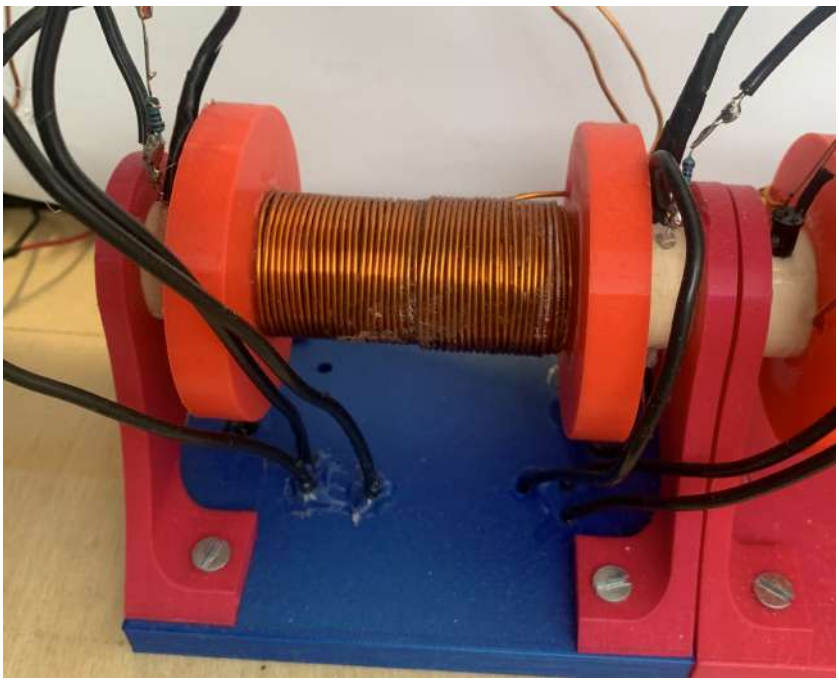

Fig. 3.5: Detail of the coil

The larger electrical components of the main power circuit, which include the diode, resistors, capacitors, IGBT and battery pack were fixed to the large sheet of plywood with bolts and nuts. Thick wires were used for interconnections to minimize resistance. Conversely, smaller components such as optical receivers and gate drivers were mounted on prototype boards and soldered.

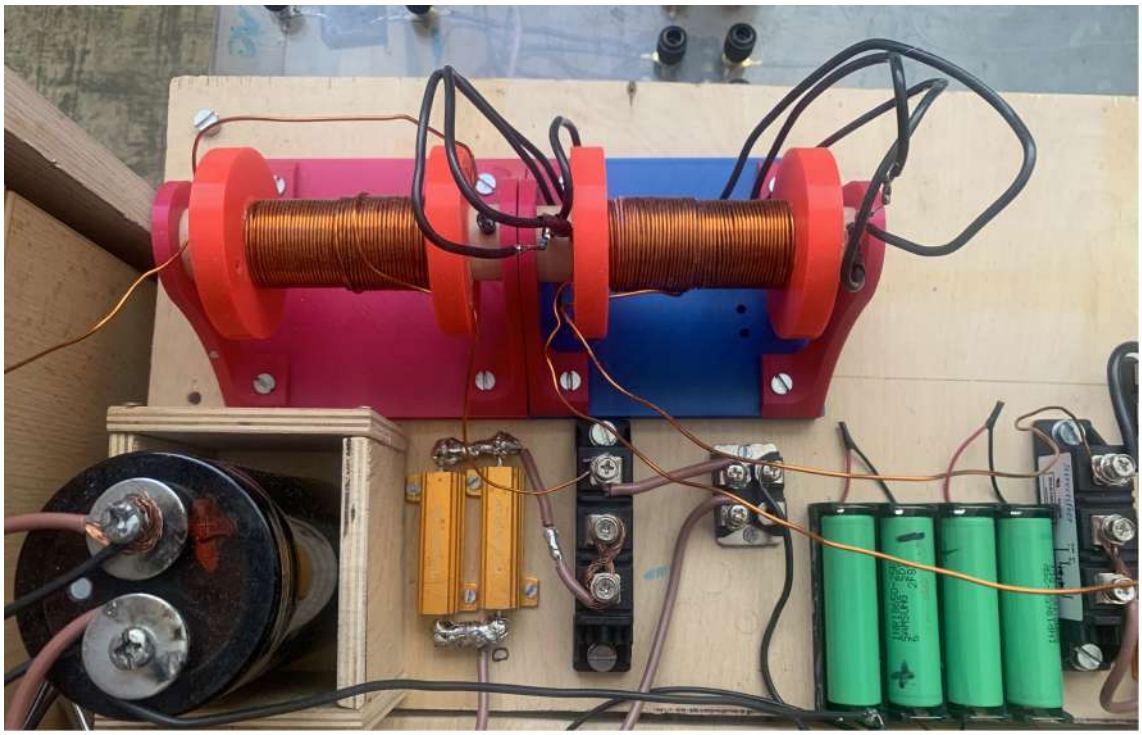

Fig. 3.6: Detail of larger components

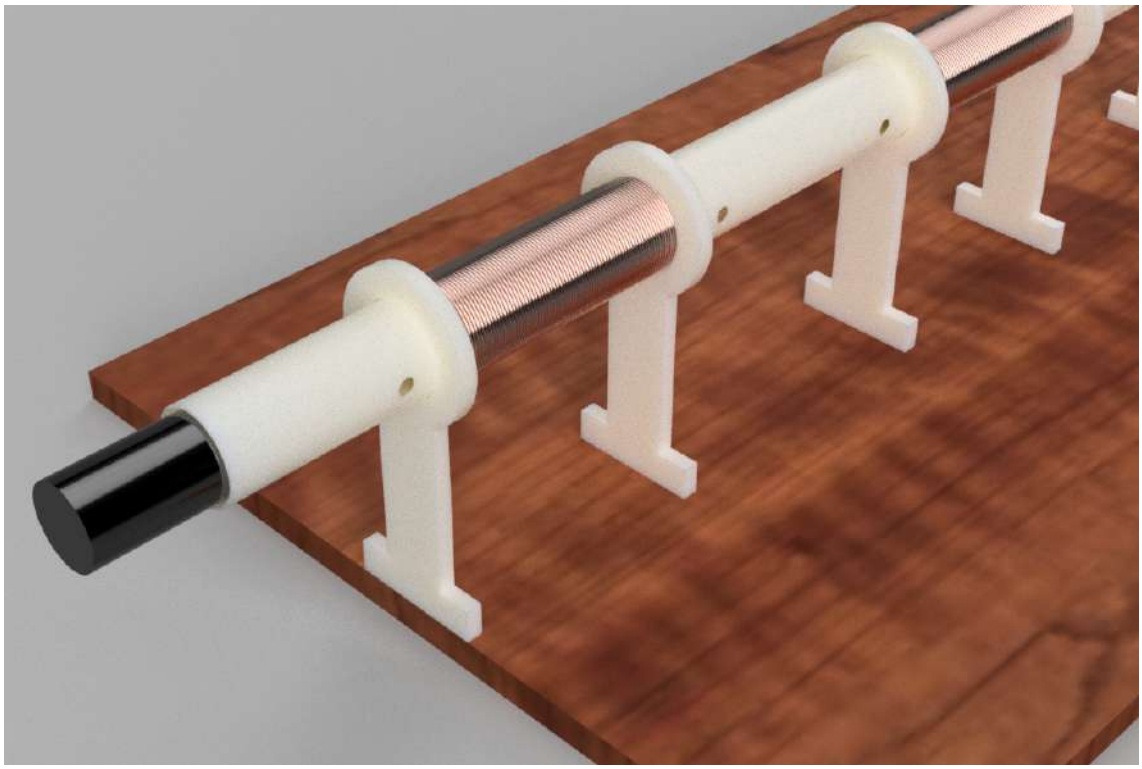

Fig. 3.7: 3D print render

3.3 Control system and sensors

Design

- FPGA: Lattice - LCMXO3D-9400HC-B-EVN

In the design of the control system for the coilgun prototype, the choice between a FPGA and a MCU was a critical decision. The FPGA was selected over the MCU primarily for the following reasons:

- Personal Experience
- Speed

To ensure complete galvanic isolation of the FPGA from the rest of the circuits, signals to and from the FPGA were transmitted via receivers and transmitters connected through optical cables. This isolation was crucial for protecting the FPGA from electrical noise, voltage spikes, and potential interference from other system components.

The timing of the system is managed through a combination of sensors and logic implemented using an FPGA. The first stage is triggered by a firing switch, which is one of the switches located directly on the FPGA board. The duration of the pulse is controlled by a shift register implemented as a counter within the FPGA, along with a state machine that determines the appropriate actions to be taken.

Sensors

- IR diode: L-34F3BT
- IR transistor: LTR-3208
- Optical Transmitter: OTJ-1
- Optical Receiver: TORX1353(F)
- Optics cable: 51217 goobay

In the control system of the coilgun prototype, optical sensors were selected due to their quick response time and high reliability. These characteristics make them ideal for precise and consistent detection in high-speed applications.

The optical sensors serve two primary functions within the system:

- Projectile Detection: When the projectile crosses a predetermined point, the optical sensor detects its presence and sends a signal to the FPGA. This signal can trigger the activation of subsequent coils, ensuring precise timing and coordination of the electromagnetic pulses required to accelerate the projectile.
- Speed Measurement: The sensors also facilitate the measurement of the projectile's speed. By detecting the time intervals at which the projectile crosses different points, the system can calculate its velocity with high accuracy.

Construction

Both the FPGA and its connected transmitters and receivers were provided with independent power supply. A power bank was utilized for this purpose, which is advantageous as it eliminates the introduction of noise from wall sockets. This setup ensures a clean and stable power source for the FPGA and associated components, thereby enhancing the overall reliability and performance of the system.

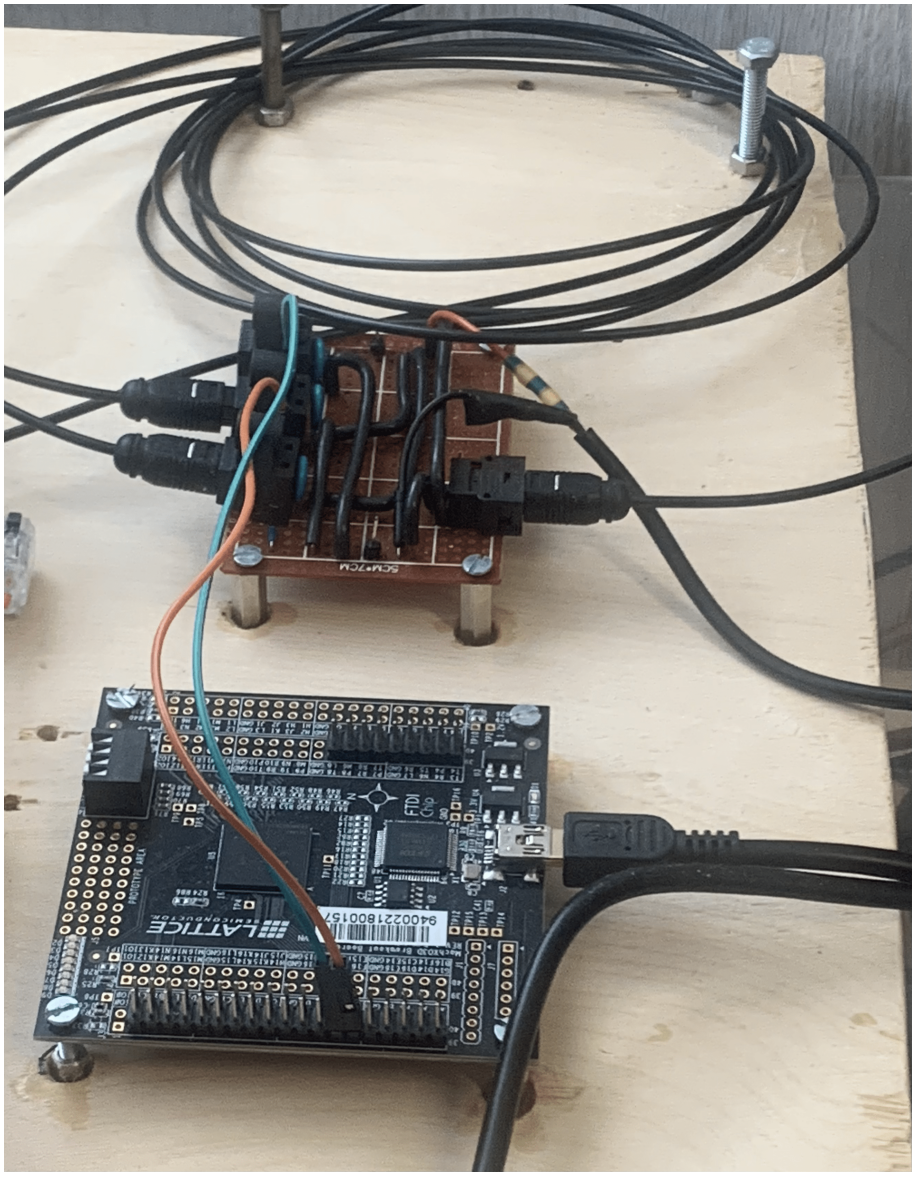

Fig. 3.8: Detail of FPGA and it's receivers, transmitters

3.4 Charging charger

Design

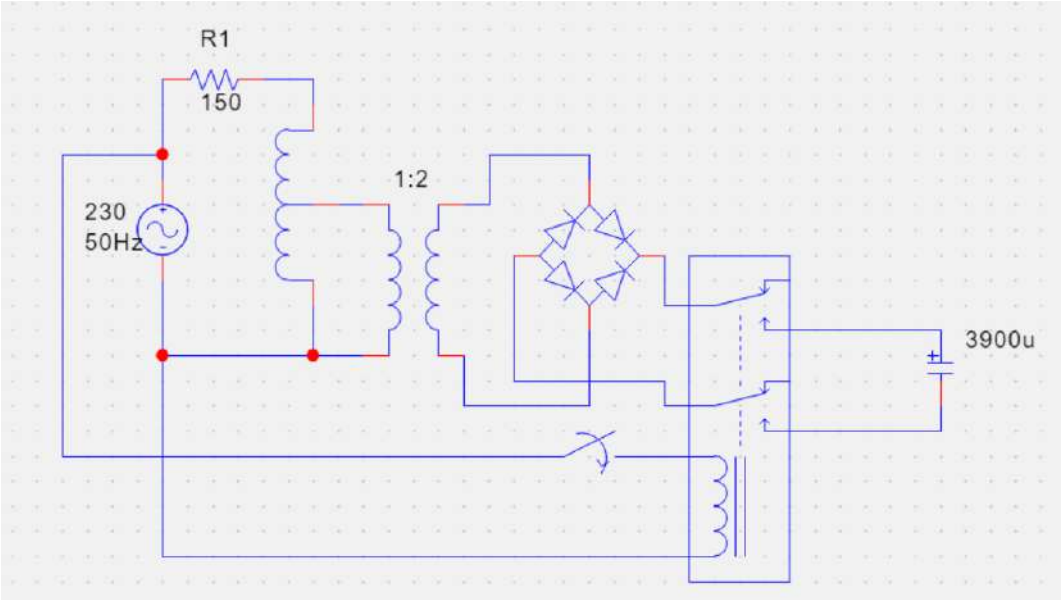

Fig. 3.9: Charging circuit

- Variac: Vevor 500VA
- Step-up transformer 1:2
- Full bridge rectifier: BR310
- Current limiting resistor: 100W 150 Ω
- Relay: 30A

Based on prior experience with high-voltage charging circuits for capacitor banks, the design of the charging circuit for this project prioritizes reliability over convenience. Although DC/DC boost converters can be small and battery-powered, offering significant convenience, they have notable drawbacks.

To address these concerns, a transformer-based charging circuit was selected. This circuit incorporates transformers and a full-bridge rectifier, chosen despite its larger physical size. The use of transformers and a full-bridge rectifier provides superior reliability and robustness, essential for the high-voltage requirements of this project. This choice emphasizes the importance of ensuring the system's reliability and safety.

The variac is connected through a current-limiting resistor to prevent potential damage. The output of the variac, which reaches approximately 280 V, is sufficient to charge the capacitors. However, to accommodate the need for higher voltages, a 1:2 step-up transformer is included in the circuit. The output of this transformer is connected directly to a full-bridge rectifier, which rectifies the voltage to produce the DC required for charging the capacitors.

The outputs of the full-bridge rectifier are then routed to the main contacts of a normally open (NO) relay. When 230 V is applied to the controlling coil of the relay, the contacts close, allowing the rectified voltage to charge the capacitors.

Construction

The entire charging circuit is mounted on a large sheet of plywood. Each component is securely fastened in place with bolts and nuts to ensure stability during transit. Threaded rods are inserted through holes at each corner of the plywood sheet, lifting it off the floor and securing it in place with nuts and washers on the rods. As depicted in Figure 3.11, wheels are attached to the bottom of the threaded rods for ease of mobility.

A second layer is placed on top of the plywood sheet holding the main components. This top layer, as shown in Figure 3.11, is constructed from PMMA, also known as plexiglass, and features a small piece of plywood on which the buttons for actuating the relay are mounted. There are a total of four buttons, enabling four stages to be connected simultaneously, with each stage capable of being charged to any desired voltage.

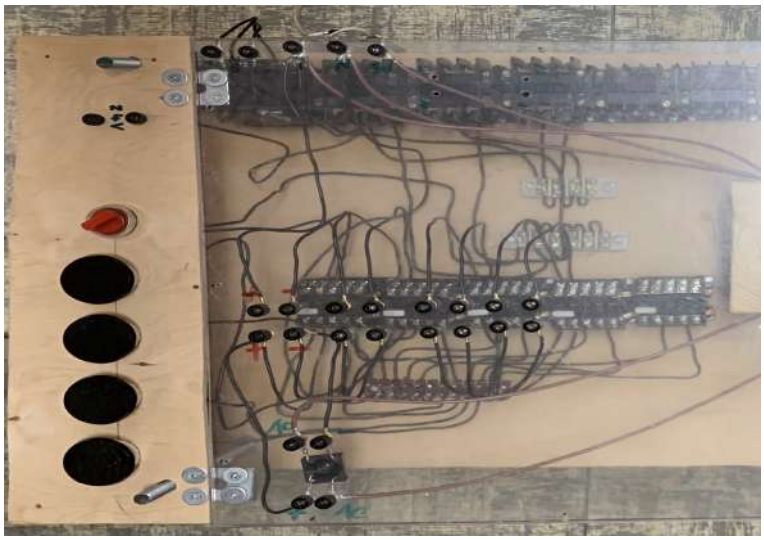

Fig. 3.10: Top detail of charging circuit

Fig. 3.11: Look at the whole charging circuit

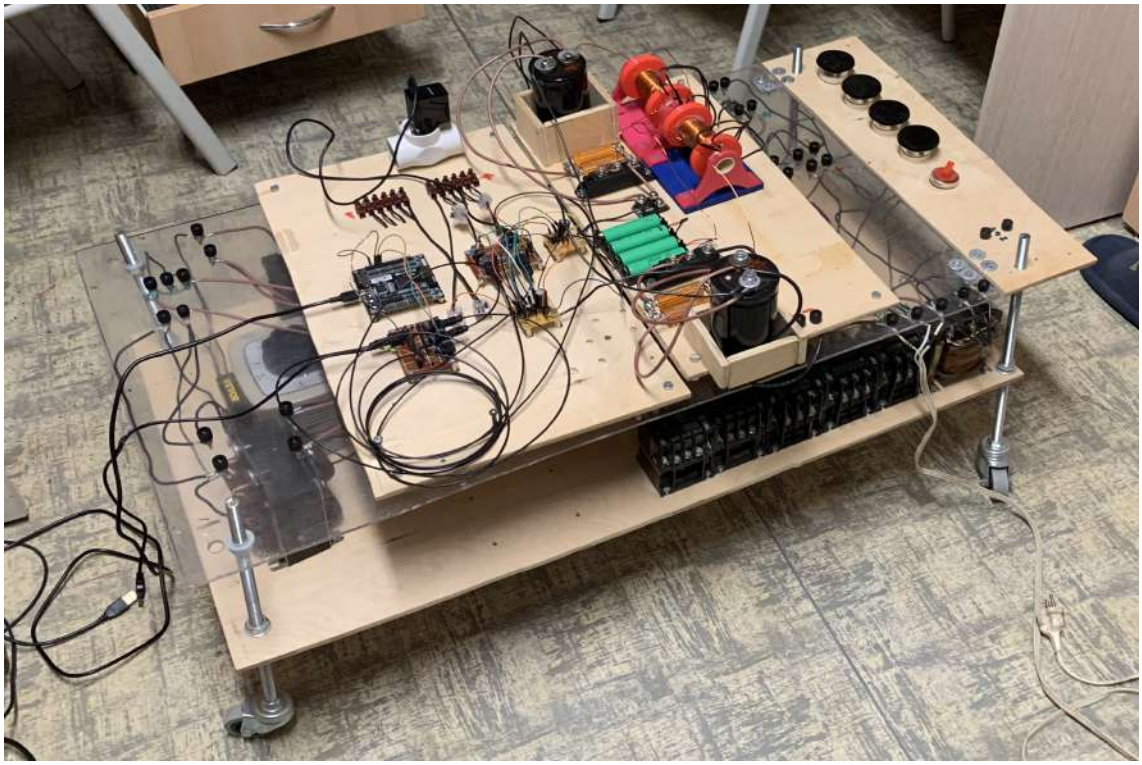

Fig. 3.12: Look at the whole prototype

4 Testing, measurements and optimalization

This chapter focuses on the critical stages that follow the initial build: testing, measurements, and optimalization. Measurements are essential to evaluate the performance of the prototype and identify any discrepancies from the expected outcomes. Coilgun efficiency is usually anywhere in the range of 0 to 6 % and with increasing muzzle velocity the efficiency decreases. [4][8]

4.1 Pulse duration

In the initial phase, it is imperative to determine the timing accurately meaning how for how long we have to turn on the IGBT. Consider the following scenario: a projectile is positioned right on the edge of a coil, resulting in a distance of 50 mm before the projectile begins to experience the suck-back effect (a retarding force that slows down the projectile). Additionally, 1 ms must be allocated for the coil to ramp down from its maximum current.

There are multiple methods to determine the appropriate pulse duration:

- Calculation: Based on theoretical models and equations.
- Simulation: Using software tools to model the behavior of the coil and projectile.
- Estimation: Making an educated guess based on prior experience and empirical data.

Let's take a educated guess. Assuming that the efficiency ranges from 1% to 6%, a simulation can be created using the known coil parameters Fig. 4.1. Also important to take into the account is as the projectile enters the solenoid, its inductance increases, leading to a decrease in peak current and a slower discharge as visible on Fig 4.2. The simulation indicates that the capacitor discharges to 200 V after approximately 2 ms, resulting in the dissipation of about 234 J of total energy from the capacitor.

Subsequently, the energy and velocity of the projectile are calculated for both efficiency scenarios. The resulting velocities are 14 m/s with 1% efficiency and 35 m/s with 6% efficiency. This initial guess can then be experimentally verified and adjusted.

Through a experiments, the initial estimate for the pulse duration was found to be inaccurate. The experiments indicated that the pulse duration needed to be shorter than initially predicted.

My best guess is that projectiles were being decelerated on their way out of the coil. This was attributed to the IGBT being turned off too late, resulting in remnant

current in the coil exerting a retarding force on the projectile.

Based on these findings, it was concluded that reducing the pulse duration would minimize the suck-back effect. By turning off the IGBT earlier, the residual current in the coil is reduced, thereby allowing the projectile to exit more smoothly and at a higher velocity.

A similar process was employed when testing different projectiles. Through experimental trials, the pulse duration was systematically adjusted to achieve optimal performance for each type of projectile.

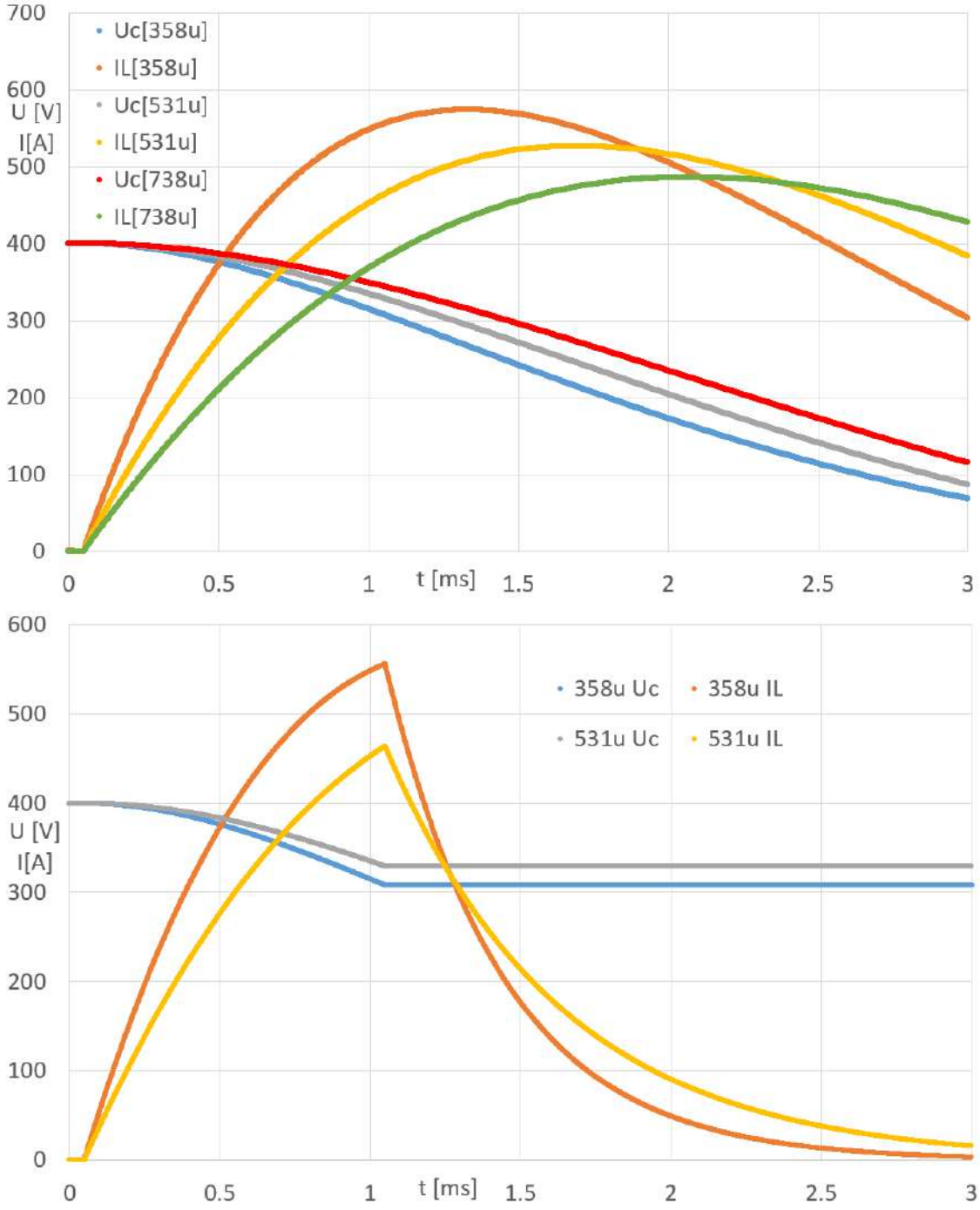

Fig. 4.1: Simulation showing the effect of changing inductance as projectile enters the coil.

4.2 Experimental results

In Table 4.1, the best cases of measured velocity and efficiency for each projectile are presented. The initial capacitor voltage was not consistently 400V; it sometimes varied above or below this value. Similarly, the voltage after discharge was not always 300V; it also varied. These fluctuations could have impacted the recorded efficiencies.

Table 4.1: Parameters and measurements for all types of projectiles

Projectile	1	2	3	4	5	6
m [g]	26	28	18	13	15	24
l [mm]	47	51	34	39	28	41
d [mm]	10	10	9	8	12	12
Material	Steel	Steel	Steel	Steel	Ferrite	Ferrite
v_{max2} [m/s]	13.97	13.39	11.68	16.77	19.17	19.31
η_{max2} [%]	0.93	0.92	0.45	0.67	1.01	1.64
E_{k2} [J]	2.53	2.51	1.22	1.82	2.75	4.47
v_{max1} [m/s]	11.13	10.54	10.87	14.27	14.14	14.7
η_1 [%]	1.18	1.14	0.78	0.97	1.1	1.9

- Material - Steel:Fe78.5Zn21 Ferrite:Fe69.5Mn21.4Zn9
- v_{max2} - Maximal muzzle velocity using two stages.
- η_{max2} - Maximal efficiency reached using two stages
- E_{k2} - Kinetic energy of projectile
- v_{1max} - Maximal muzzle velocity using single stage.
- η_1 - Maximal efficiency reached using single stage.

Fig. 4.2: Experimental projectiles

$$\eta_{max2} = \frac{E_k}{E_{used}} = \frac{\frac{1}{2} * m * v^2}{(E_{400V} - E_{300V}) * 2} = \frac{\frac{1}{2} * m * v^2}{(\frac{1}{2} * C * V^2 - \frac{1}{2} * C * V^2) * 2}$$

$$= \frac{\frac{1}{2} * 24 * 10^{-3} * 19.31^2}{(\frac{1}{2} * 3900 * 10^{-6} * 400^2 - \frac{1}{2} * 3900 * 10^{-6} * 300^2) * 2} * 100 = 1.64\%$$

The results presented in Table 4.1 indicate a decline in efficiency with the introduction of a second acceleration stage. This outcome was anticipated due to several factors inherent to multi-stage coilgun.

- Increased Projectile Speed: When the projectile enters stage 2, its velocity is higher compared to its velocity upon entering stage 1. Consequently, the duration available for each stage to impart acceleration is reduced. This abbreviated acceleration period may result in sub-optimal energy transfer. Additionally, there is an increased risk of the "suck-back" effect.
- Imperfect Timing: Improper timing in the energization of the coils can lead to either premature or delayed activation. This mistiming hinders the provision of optimal acceleration, thus diminishing the overall efficiency of the system which is already low. This issue arises from the substantial variability in the projectile's speed between stages. To address this, implementing two light gates between stages can measure the projectile's speed and relay this information to the control system. This feedback would allow the system to adjust the timing accordingly, enhancing the accuracy and efficiency of the acceleration process.

A typical pistol bullet weighs around 8 grams and travels at a velocity of 360 m/s, yielding kinetic energy of approximately 500 J. In order to attain a kinetic energy of 500 J with this coilgun, the calculation is based on the assumption of the best-case scenario, where the efficiency of a single stage is 1.9% and it stays the same even for the following stages. This efficiency translates to an energy transfer of 2.6 J per stage. Therefore, to achieve a total energy of 500 J, it would necessitate the utilization of 193 stages.

5 Conclusion

The primary objectives of this bachelor thesis were to study the physical principles and working mechanisms of a reluctance coilgun, analyze various factors affecting its performance, and design, construct, test, and optimize a two-stage prototype. Through comprehensive theoretical analysis and practical experimentation, these goals were successfully achieved.

The thesis began with an in-depth exploration of the fundamental theory behind the function of coilguns. This included detailed explanations of electrical induction, magnetism, and magnetic fields, laying the groundwork for understanding the operation of electromagnetic launchers. Following this, the working principles of three major types of electromagnetic launchers—railgun, inductance coilgun, and reluctance coilgun—were examined. The discussion also delved into the challenges faced during coilgun design, such as the choice of switching devices (mechanical switches, thyristors, or IGBTs), and the trade-offs associated with each option.

The third chapter focused on the selection of key components and the construction of a two-stage prototype. This involved designing the main power circuit, control system, and sensors, as well as addressing issues related to pulse duration and timing. The prototype's construction was followed by extensive testing and optimization, documented in the fourth chapter. The testing phase highlighted the challenges of achieving optimal efficiency in a multi-stage coilgun, particularly regarding timing accuracy and energy transfer.

Experimental results demonstrated a decline in efficiency with the addition of a second acceleration stage, primarily due to increased projectile speed and the resulting shorter acceleration period per stage. This was anticipated and attributed to factors such as imperfect timing in coil energization and the "suck-back" effect. To mitigate these issues, the implementation of a feedback system using light gates to measure projectile speed and adjust timing was recommended.

In conclusion, this thesis successfully met its objectives by providing a detailed theoretical framework, addressing practical design considerations, and constructing and optimizing a functional two-stage coilgun prototype. The insights gained from this research contribute valuable knowledge to the field of electromagnetic launchers and offer a foundation for further improvements in coilgun efficiency and performance.

All the goals outlined at the beginning of this thesis have been completed.

Bibliography

[1] FEYNMAN, Richard P., Robert B. LEIGHTON, and Matthew SANDS. *Feynman Lectures on Physics*. Vol. II. Basic Books, 2011. ISBN 9780465024940.

[2] HANSON, Barry. *Practical Coilgun Design*[online] 2012. Available from: https://coilgun.info/theoryinductors/home.htm [cit. May 2024].

[3] GRIFFITHS, David J. *Introduction to Electrodynamics*. Fourth Edition. Cambridge University Press 2021. ISBN 9781108420419.

[4] DENG, Hui-min, Yu WANG, Fa-long LU, and Zhong-ming YAN. *Optimization of reluctance accelerator efficiency by an improved discharging circuit.* Defence Technology 16, no. 3 (2020): 662-667.

[5] El-HASAN, TAREQ S. D*esign of a single stage supersonic reluctance coilgun (RCG).* 2011 IEEE pulsed power conference. IEEE, 2011.

[6] ORBACH, Yafit, Matan OREN, and Moshe EINAT. *75 m/s simulation and experiment of two-stage reluctance coilgun.* Journal of Mechanical Science and Technology 36, no. 3 (2022): 1123-1130.

[7] KAYE, Ronald J., et al. *Design and evaluation of coils for a 50 mm diameter induction coilgun launcher.* IEEE Transactions on magnetics 31.1 (1995): 478-483.

[8] EINAT, MOSHE, and Yafit ORBACH. *A multi-stage 130 m/s reluctance linear electromagnetic launcher.* Scientific Reports 13.1 (2023): 218.

[9] MARSHALL, Benjamin. *Coil Gun Design Guide*[online] 2021. Available from: https://bitly.cx/D7rb [cit. May 2024].

[10] Accel Instruments *Magnetic Field Calculator for Coils and Solenoids*[online] 2022. Available from: https://www.accelinstruments.com/Magnetic/Magnetic-field-calculator.html [cit. May 2024].

Symbols and abbreviations

TBD	To be determined
NA	Not applicable
E (V/m)	Electric field
B (T)	Magnetic field
H (A/m)	Magnetic field strength
F (N)	Force
I (A)	Electric current
q (C)	Electric charge
v (m/s)	velocity
θ **(°)**	angle
j $(\mathbf{A}/m^2)$	Current density
ϕ **(Wb)**	Magnetic flux
χ **(-)**	Magnetic susceptibility
μ **(H/m)**	Permeability
μ_0 **(H/m)**	Permeability of free space
μ_r **(-)**	Relative permeability
M (A/m)	Magnetization
j $(\mathbf{A}/m^2)$	Current density
c (m/s)	Speed of light
ϵ **(F/m)**	Permittivity
ϵ_0 **(F/m)**	Permittivity of vacuum
$\mathcal{E}$ **(V)**	Electro motive force
ρ $(\mathbf{C}/m^3)$	Volume charge density